U S
University of Stavanger

Faculty of Science and Technology

MASTER'S THESIS

Study program/ Specialization: **Offshore Technology/Subsea and Marine Technology**	Spring semester, 2014 <u>Open</u> / Restricted access
Writer: **Almaz Khatmullin**	.... (Writer's signature)

Faculty supervisor: **Professor Ove Tobias Gudmestad,**

Professor Anatoly Borisovich Zolotukhin

External supervisor(s): **Mikhail Mosesyan, Lukoil Overseas North Shelf AS**

Thesis title: **Technological challenges and possible solutions for drilling operations in the Great Barents region**

Credits (ECTS): 30

Key words: platform design, standards, ice loads.	Pages: 97 Stavanger, 15.06. 2014

ABSTRACT

The Barents Sea region is thought to play a key role in Russian and Norwegian oil and gas field development and hydrocarbon resources production. Both countries are moving petroleum activities into the Barents Sea Area due to the high potential of hydrocarbon occurrence. The relationship between Russia and Norway in the energy sphere has been peaceful and cooperative. Moreover, new perspectives for oil and gas explorations have been opened, since the signing of the agreement on a delimitation line in the Barents Sea between the two countries in 2011.

Starting with a description of the metocean conditions of the Barents Sea, the thesis will discuss the challenges for development of potential hydrocarbon fields in the Barents Sea Area. Main accent in the presented Master thesis will be placed on a review of the technological challenges for drilling operations, by providing a comparison of different International Safety Standards and Technical Regulations relevant for the Arctic region, in particular, for the Barents Sea Area including follows:

- American Petroleum Institute (API);
- International Organization for Standardization (ISO);
- Norsk Sokkels Konkurranseposisjon (NORSOK);
- Federal Agency on Technical Regulating and Metrology (Russian Federation);
- Other relevant standards.

As well, risky scenarios during drilling operations in the Barents Sea will be analyzed to ensure well control and integrity and environmental safety. Design according to different standards will be compared.

Based on a review of possible technical solutions for drilling operations in the Barents Sea Area, conclusions regarding using different Safety Standards and Technical Regulations will finally be given.

CONTENT

LIST OF FIGURES

LIST OF TABLES

ACKNOWLEDGMENTS

INTRODUCTION

The Arctic continental shelf is believed to be the area with the highest unexplored potential for oil and gas as well as for unconventional hydrocarbons.[15]

This has provoked a strong reaction and a huge interest in the High North. The Barents Sea in particular is one of the areas where it is expected to find large petroleum resources.[17]

Hence, major international energy companies are now mobilizing their resources, improving competence and knowledge, developing technology and internal regulations to prepare for a long lasting and challenging journey to the north. [18]

Estimates of undiscovered resources (see Table 1) are based on the Norwegian Petroleum Directorate's knowledge and on information from the industry's exploration of the Norwegian Continental Shelf and are presented as the expected (average) value, low estimate (P95) and high estimate (P05) in million scmoe. [13]

The Norwegian Petroleum Directorate calculates that 1025 to 6610 million scmoe remain to be discovered on the Norwegian Continental Shelf, with an expected value of 2 980 million scmoe. [13]

The Barents Sea in particular covers large areas with little data and no exploration wells, thus making the uncertainly particularly high. [17] It is estimated that there are between 245 and 2475 million scmoe. of undiscovered recoverable oil equivalents in the Barents Sea. Regarding Barents Sea South East and, there are between 55 and 565 million scmoe. of undiscovered recoverable oil equivalents.

Table 1. Undiscovered recoverable resources broken down by area on Norwegian continental shelf. [13]

Area	Low/ P95	Expected average	High / P05
North Sea	485	850	1315
Norwegian Sea	240	780	1795
Barents Sea	245	960	2475
Barents Sea South East	55	300	565
Jan Mayen	0	90	460
NCS total	1025	2980	6610

Growing oil and gas activity will entail new environmental challenges in marine areas with vulnerable ecosystems.[16]

Development of hydrocarbon fields in the Barents Sea poses considerable challenges for the Operator and involves considerations related to:

- extreme climatological statistics
- offshore structures which can resist the loading
- efficient gas or oil transportation systems
- protection of the vulnerable Arctic ecosystem
- including wildlife and fisheries
- human behavior during extreme climatological conditions (darkness, low temperature)
- economical attractive development schemes including efficient project management
- selection of technology most attractive for the Operator and the country. [3]

LIMITATIONS OF THE REPORT

This Master Thesis takes into consideration the Norwegian sector of the Barents Sea (Figure 1) north of the Norwegian mainland, south of Bear Island (Bjørnøya) and prolongs eastwards in the direction of the Norwegian/Russian border (indicated with red solid line) that came into effect in 2011. This area corresponds approximately to the area that is open for exploration and exploitation of oil and gas resources in the Norwegian sector of the Barents Sea.
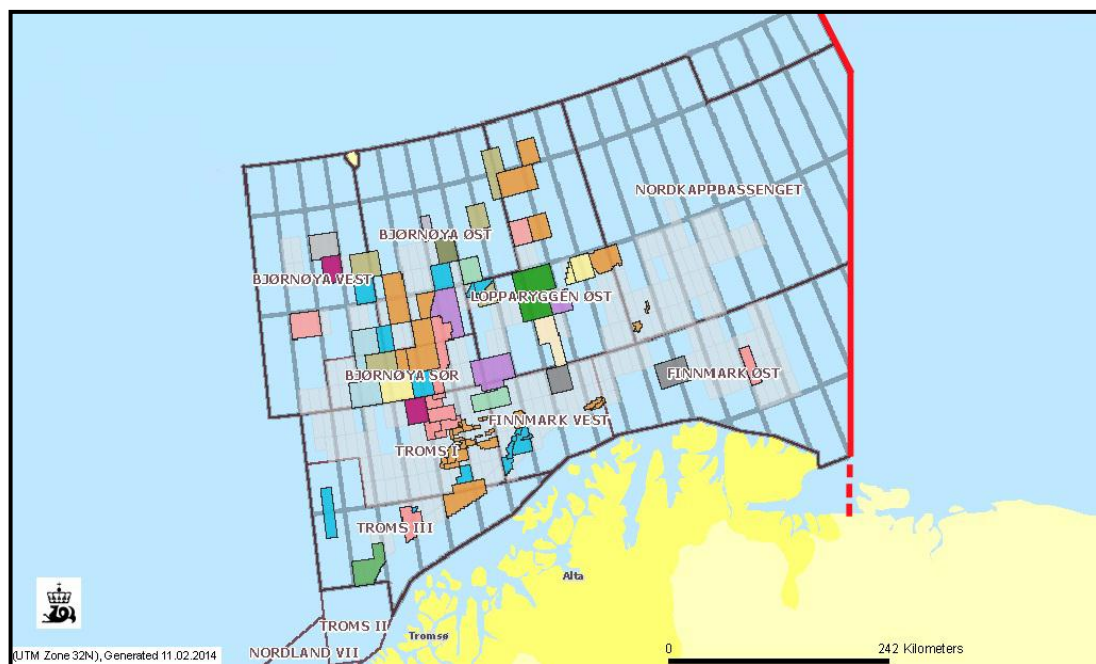
Figure 1. Map of the area and the Norwegian/Russian border.

The main interest of this report is accented at two licenses of Lukoil Overseas North Shelf AS. Based on the results of the 22nd licensing round conducted by the Norwegian Ministry of Oil and Energy, LUKOIL was awarded partnership in two licenses in the Norwegian sector of the Barents Sea.[8]

Figure 2 illustrates block 719(Fingerdjupet Region) and block 708(Finnmark Region) situated in the Barents Sea. Block 719 is belonged to LUKOIL with 30%interest, Britain's Centrica (operator) holds 50%, Norway's North Energy - 20%. At block 708 LUKOIL holds a 20% interest, Sweden's Lundin Norway (operator) - 40%, NorthEnergy - 20% and Italy's Edison - 20%.
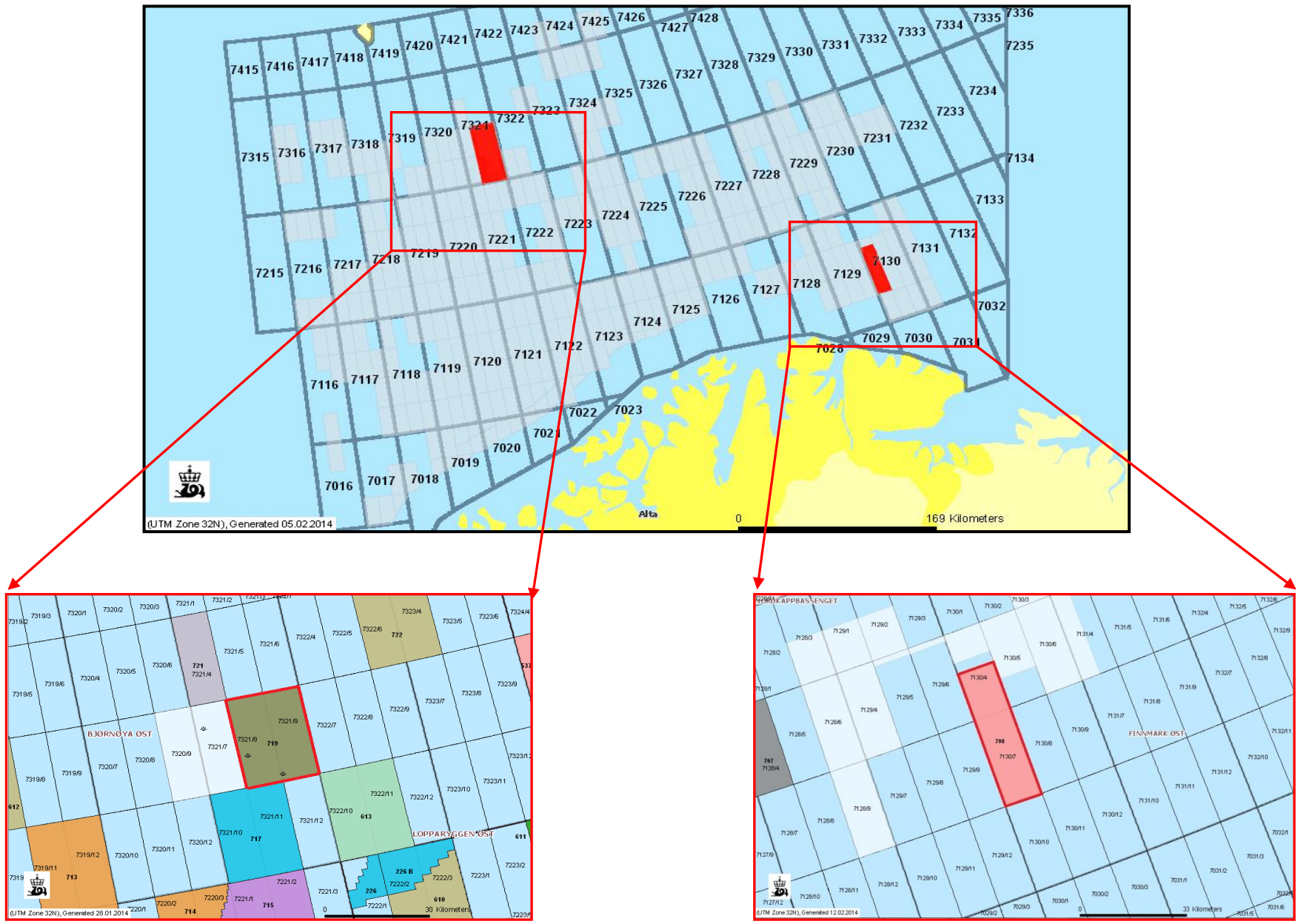
Figure 2. Lukoil Overseas North Shelf As's licenses at block 719 and block 708. [14]

CHAPTER 1.TECHNOLOGICAL CHALLENGES FOR DRILLING OPERATIONS IN THE BARENTS SEA

1.1. Exploration activity in the Barents Sea

Exploration activities have been pursued in the Norwegian sector of the Barents Sea since the fifth licensing round in 1980.[13] Since 1980 to 2014 (January) 102 exploration wells have been drilled, of which 88 are wildcats, 17 are appraisal wells. See appendix A.

The first Exploration well 7120/12-1 was spudded with the semi-submersible installation Treasure Seeker on 1st June 1980. The well was permanently abandoned as dry with weak shows on 12th October 1980.[14]First discovery – 7120/8-1 (Askeladd) – followed in 1981. More than 30 discoveries have been made in the Barents Sea. [13]

Optimism was high in the early 1980s, when several gas discoveries were made in the Hammerfest Basin. A number of wells drilled outside that basin after 1986 were either dry or contained only small gas resources. [13]

Due to declining of exploration interest, from 1994 to year 1999 inclusive not a single well was drilled in the Barents Sea. (See Appendix A)

Since 2000 to 2014 (January) 52 exploration wells have been drilled, of which 41 are wildcats, 11 are appraisal wells. (See Appendix A)

1.2. Production activity in the Barents Sea

Oil and gas operations have been pursued in the Barents Sea for more than 30 years, only one field has come on stream – Snohvit, which comprises eight gas discoveries. The Goliat oil field is also under development. [13]

The Snøhvit unit includes the Snøhvit, Albatross and Askeladd structures. The approved PDO for the gas resources includes subsea templates for 19 production wells and one injection well for CO^2. [14]

In 2005 in the Snøhvit field 8 production wells have been drilled, and in 2006 – 1 producer. As well, in order to maintain reservoir pressure 1 injection well has been drilled in 2004.

Goliat will be developed with a circular FPSO (Sevan 1000) including eight subsea templates with a total of 32 well slots. The subsea templates will be tied back to the FPSO with an integrated storage and loading system.[14]

Based on Norwegian Petroleum Directorate's Fact Pages 3 injection and 1 observation wells have been drilled in the Goliat oilfield in 2013. Production is planned to start late in 2014. [14]

As a curiosity it can be mentioned that the exploration well drilled furthest from mainland Norway in the Barents Sea was operated by Norsk Hydro using Polar Pioneer in 1992 on block 7316/5-1. The well location was 73.51997°N, 16.43325°E, ca 217 NM or 402 km from Hammerfest.[9]

1.3. Conditions in the area

1.3.1. Geography

The Barents Sea covers an area comparable to 7-8 times the size of the North Sea. The area is characterized by the fact that it lies to the far north and that areas are covered by ice for parts of the year.[4]

Nowadays, there are lots of different definitions of the limitations of the Barents Sea borders. Based on the "Limits of Oceans and Seas" paper by International Hydrographic Organization, the Barents Sea (Figure 3), situated off the north-eastern coast of Norway and the north-western coast of Russia, is bounded by Svalbard (Spitsbergen and Nordaustlandet) on the Northwest, by Zemlya FrantsaIosifa Archipelago (Franz Josef Land) on the Northeast, and by Novaya Zemlya on the East (indicated with blue line). [1]

However, according to the Norwegian Petroleum Directorate the west border of the Barents Sea starts from 69°N 16°E up to 72°N 16°E and continuous from 72°N15°E to Sørkapp on Svalbard (indicated with red line)

Figure 3. Barents Sea. [1]

The Barents shelf is rather deep. In the Barents Sea more than 50% of the area has depths of 200-500 m. The average depth is approximately 200 m and the maximum depth in the Norwegian trench reaches 513 m and in the Franz Josef Land straits depth exceeds 600 m. [2]

1.3.2. Climate

Due to the warm ocean currents, the Barents Sea has a climate which is much milder than comparable areas at the same latitude. This applies particularly to the sea and air temperature, but in the winters the conditions are more hostile than at other parts of the Norwegian Continental Shelf. [3]

The main climate-forming factors are latitudinal changes in the incidence of solar radiation and the influence of the warm Atlantic water masses, entering the Barents Sea in the west. In the terrestrial part of the region the climate is transitional from marine to continental, with the continental influence increasing with distance from the coast. The climatic impacts of increasing continental influence are decrease in cyclonic activity, increased range of air temperature, and decrease in number of cloudy days and days with precipitation. [2]

1.3.3. Temperature conditions

Compared to all the Arctic seas the Barents Sea climate is characterized by high air temperatures, mild winters and high precipitation. The severity of the climate, based on average data, increases in the sea from north to south and from west to east.[5]
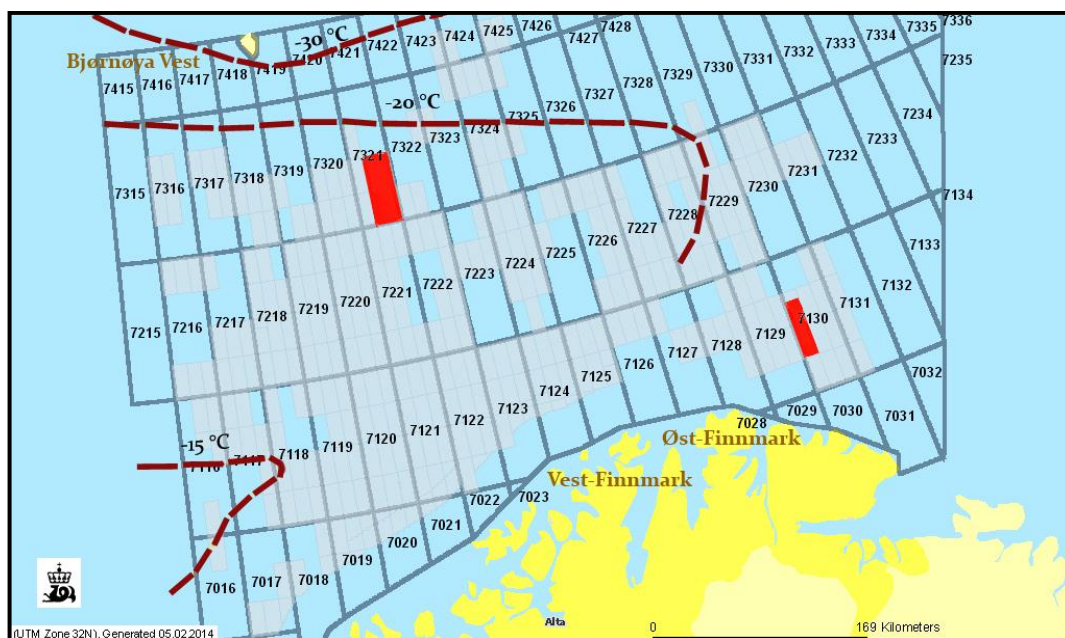
Figure 4. Lowest air temperature with an annual probability. [10]

The average annual temperature is characterized by the following values: Bjornoya -1.6 ° C, Barentsburg (Spitsbergen) -5.2 °C, Quiet Cove -10.5 °C. Average temperatures of the coldest months on the coast equals: -10 °C, -15 °C, on the northern islands -20 °C, -22 °C. Monthly average temperatures in the central area vary from -4 to -10 ° C in winter and from 3 to 5 ° C in the summer, in the south - eastern region from -15 to -20 °C in winter and from 1 to 3 °C in summer.[5] The minimum air temperatures are shown in Figure 4.

1.3.4. Waves

Figure 5, from [Norsok, 2007], shows the significant wave height with an annual probability of exceedance of 10^{-2} for sea-states of 3 hours duration in the Western and South Western Barents Sea.
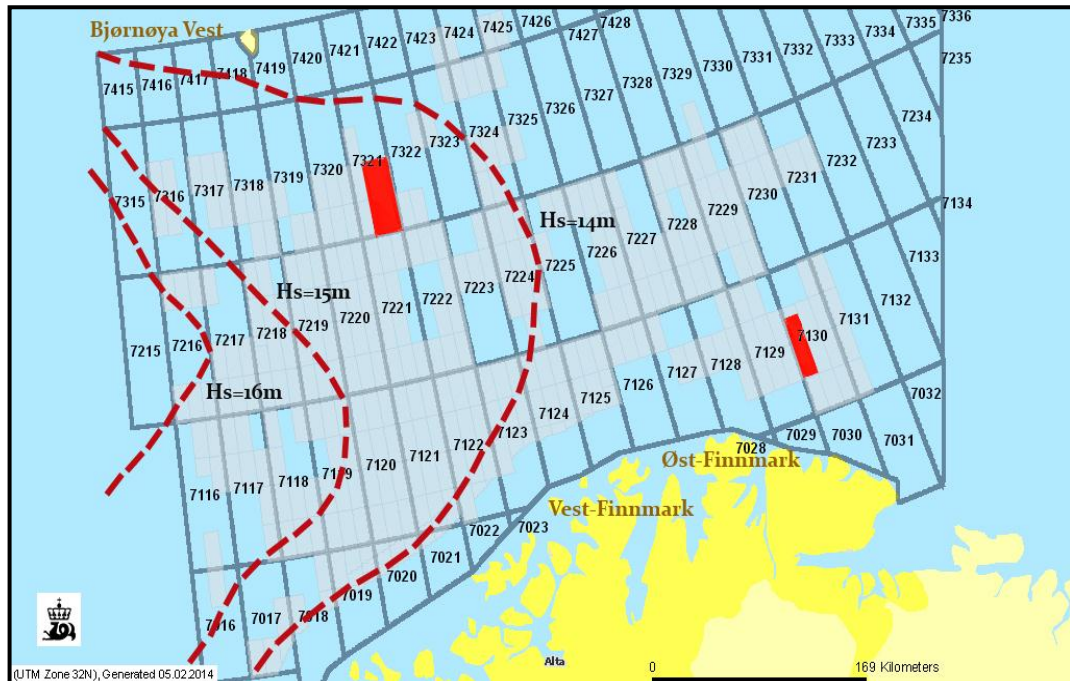
Figure 5. Significant wave height Hs with annual probability greater than 10-2 for sea-states of 3hour duration. [10]

Iso-curves for wave heights are indicated with dotted lines. It can be noted that the design wave conditions are similar to other areas on the Norwegian Shelf.[6]

At Tromsøflaket the wave periods corresponding to a 100-year wave height will be higher (17-19 sec) than what is usual in the North Sea (15-17 sec).

During the drilling with Ross Rig on 10 November 1988 near Bjørnøya, the wave period reached 18 seconds. This was very close to the resonance period of 20.3 seconds for the platform. This high wave period resulted in drilling stoppage for 8 hours. [12]

1.3.5. Wind

If we look at measurements carried out at several offshore locations and extrapolate them to an annual probability of exceedence of 10^{-2}, the result will be 30 - 36 m/s at a height of 10 m, and averaged over 10 min. [12]

Use of hindcast data from Bjørnøya, Sentral-banken and Nordkappbanken gives approximately the same extreme values as for Tromsøflaket.[12]

In the guidelines (1987), a recommended value of 41 m/s is suggested for the whole Norwegian continental shelf. The recommendation should be on the safe side as far as the Barents Sea is concerned. This means that those who want to use other values may do so.[12]

1.3.6. Polar Lows

Polar low pressures, which are mainly encountered in the period from September to early summer, are of concern as they could limit operational time for construction work. The Polar Lows are small, rather intense low pressure systems in the Arctic. Polar Lows are a rare special case of strong troughs, there are, however, lack of models and data to predict these polar lows. Their characteristics are as follows:

· formed at sea in cold air outbreaks winter time
· often having rapid development
· gale or storm force winds, seldom hurricane
· heavy snow showers, icing, changing wind direction
· life span 6h to 1-2 days
· diameter 100 - 500 km[6]

A NOAA-9 polar orbiter satellite's image (figure 6) (visible band) shows a polar low over the Barents Sea on 27 February 1987. The southern tip of Spitsbergen is visible at the top of the image. The polar low is centered just north of the Norwegian coast. [22]

Based on a report of Noer and Lien [7] the polar lows have been observed from 2000 to 2010. Synoptic observations and daily registrations have been made at the Norwegian Meteorological Institute in Tromso. Focus of registrations has been made mainly from the Greenland east coast to Novaya Zemlja and from 65°N to the Arctic ice edge.

As regards to the design of platforms, polar low pressure is not a significant problem. It will not give increased extreme estimates of wind speed, wave height, air temperature or icing. [12]
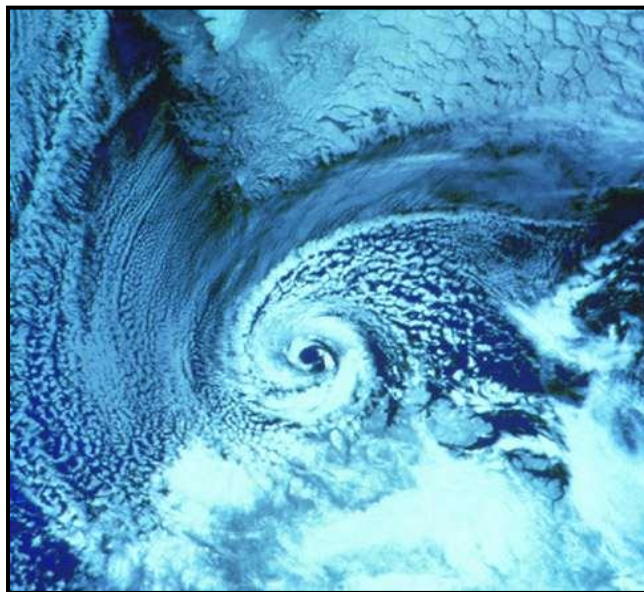
Figure 6. Polar low over the Barents Sea on February 27, 1987. [22]

On the other hand they create problems for operations and planning of operations for a long period of time, as is normal for other places on the continental shelf. One example is Norsk Hydro's drilling on Block 7321/9 in the autumn of 1988. Two polar storms resulted in drilling stoppage for 22 hours. [12] Exploration drilling platforms designed in accordance with Norwegian rules with a recommended wind speed value of 41 m/s are not expected to have difficulties in the Barents Sea.[12]

Figure 7 shows the latitudes and longitudes of 29 polar lows that have been registered in the 11 winter seasons within the limited area.

Figure 7. Polar lows registered in the Barents Sea from 2000 to 2010. [7]

1.3.7. Icing and icebergs

The seawater in the Barents Sea will freeze when the water has a temperature between -1,7°C to -1,9°C dependent on the salinity of the water. Sea ice with a return frequency of 100 years normally only occurs north of 73°N and to the east of 31°E.[9] The return frequency for sea ice increases to ca. 10 years at 74°N and 33°E. Icebergs have been observed at the coast of Norway a few times:

a) The first report of icebergs in the Barents Sea south of 74°N is in February 1881. Two icebergs reached the coast at Kvaløya in Troms at 70°13'N 19°30'E. The larger iceberg of the two was 7 metres high.

b) In June 1881 several icebergs were observed at Gamvik, Berlevåg and Syltefjord at East- Finnmark. The largest iceberg was enormous, with a length said to be 10 km, and a sail height of 30 m.

c) During the period of April-June 1929, a number of icebergs reached the coast of Kola Peninsula and eastern Finnmark (from 24° to 44° E). The local newspapers in Finnmark reported that they reached up to 30 metres above sea level.

d) In 1939 two icebergs were observed at Koi-fjorden close to Gamvik.[12]

The map in figure 8 contains information from Norsok N-003 source. The solid lines to the left/west indicate the annual probability of sea ice (white) and icebergs (blue) [10]
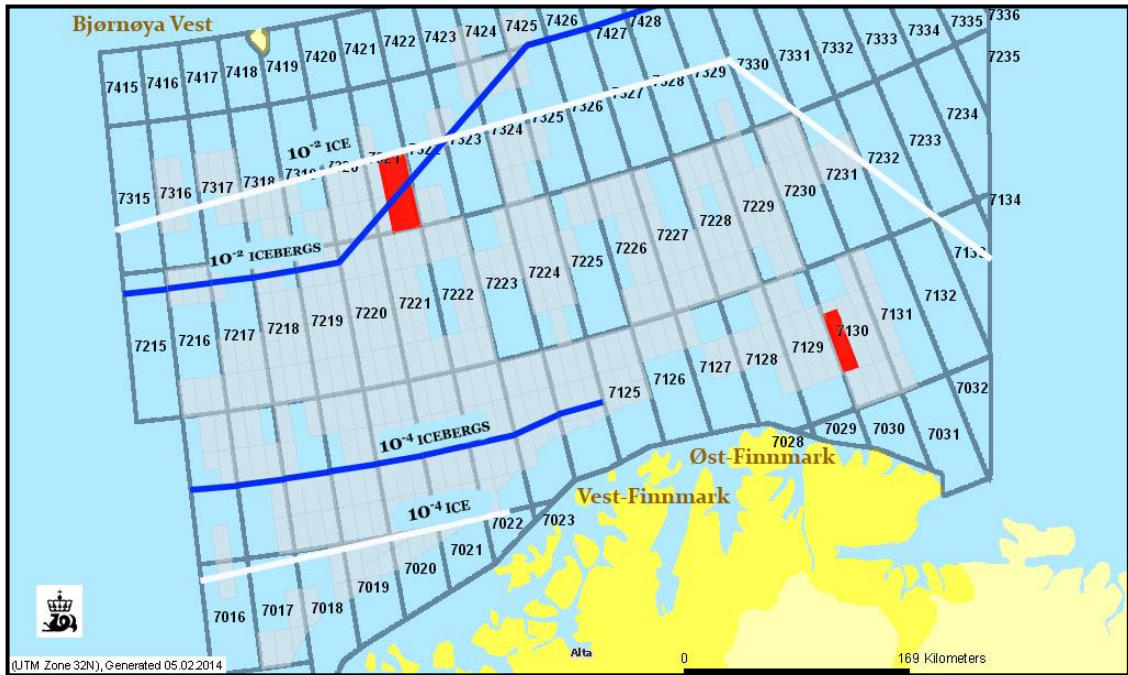
Figure 8. Limits of sea ice in the Barents Sea with annual probability of exceedance of 10^{-2} and 10^{-4}(white line) and limit for collision with icebergs with a probability of exceedance of $10^{-2}$and 10^{-4}(blue line). [10]

Although the Norwegian area currently opened for exploration is considered an ice-free area, developments will need to consider actions of sea ice and icebergs for design loads in order to meet the acceptance criteria of annual exceedance of 10^{-4}[9]. In the case of an installation to be located in an area where ice may develop or drift, consideration of ice conditions and their possible effects on the Subsea Production System should be made. The ice conditions should be studied with particular attention to possible:

i.   ice forces due to floating ice

ii.   potential scour due to grounding icebergs

iii. ice problems during the installation operations[12]

Icebergs could pose a risk to future oil and gas structures in the Barents Sea. The forces are very large, and colliding with an iceberg is almost the same as colliding with a rock. [11]The damage potential of sea ice depends on various parameters.

The most important ones are the thickness of the ice, the relative velocity between ice and platform, the physical ice properties, and the size of the ice-fields [12]

This could mean that production units should be considered designed for disconnection in the event of icebergs. [6]

1.3.8. Visibility

Visibility can be impaired by fog, rain and snowfall. Statistically this can occur for a large number of days during the year. Typically there are 64 days per year with visibility below 2km due to snow and 76 days per year with visibility below 1km due to fog. [19]

Fog in the Arctic is caused by high air relative humidity. Arctic fog is a cloud over the sea which is formed when very cold air moves over warmer water.

In winter, the frequency of fog is low because of the lower absolute humidity of water masses and a small number of condensation particles. In places where enough particles of condensation occur, frost fog can be observed.[20]

In summer over the northern Arctic Sea, the air is very close to the point of saturation by water vapor, and a small decrease in temperature is enough for fog to form.[20]

At Fruholmen, the horizontal visibility is less than 1000m for 1,51% of the year and less than 10000m for 6,76% of the year. At Bjørnøya the horizontal visibility is less than 1000m 8,58% of the year and less than 10000m 31,76% of the year. These statistics reflect the relative high occurrence of fog in the vicinity of Bjørnøya.[21]

1.3.9. Summary of main meteorological features

A summary of the main meteorological characteristics of the Barents Sea is shown on the map in figure 9 below. In general it can be said that the wind and waves decrease when moving east while air and sea temperatures and the probability of sea ice increase when moving towards the north east.
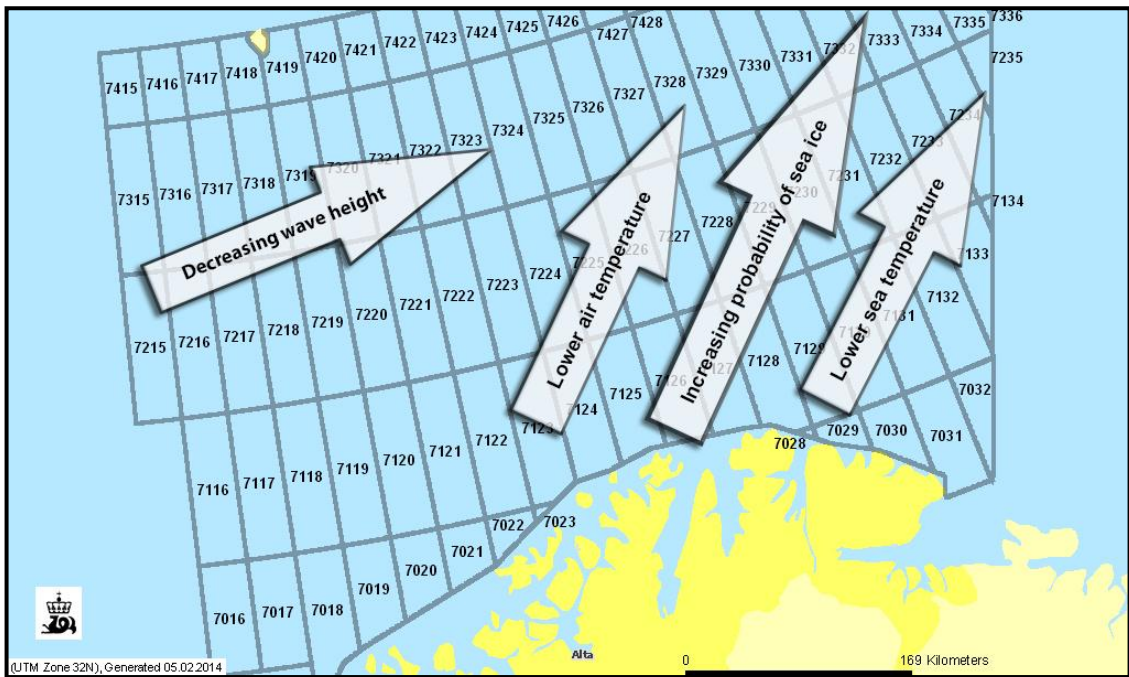
Figure 9. Summary of the main meteorological features of the Barents Sea. [14]

CHAPTER 2. COMPARISON BETWEEN RUSSIAN AND WESTERN GLOBAL ICE LOADS ESTIMATIONS CODES.

In the presented chapter are compared the most used international codes considering ice load estimations, as ISO 19906 (Petroleum and natural gas industries — Arctic offshore structures), CAN (CSA-S471-04) (General requirements, design criteria, the environment, and loads), SNIP 2.06.04-82 (Wave, Ice, and Ship Wake Loads and Effects on Hydraulic Structures), VSN-41.88 (Design of ice-resistance offshore platform).

2.1. Overview of the ISO 19906

ISO 19906 (Petroleum and natural gas industries — Arctic offshore structures)

This International Standard specifies requirements and provides recommendations and guidance for the design, construction, transportation, installation and removal of offshore structures, related to the activities of the petroleum and natural gas industries in arctic and cold regions. Reference to arctic and cold regions in this International Standard is deemed to include both the Arctic and other cold regions that are subject to similar sea ice, iceberg and icing conditions. The objective of this International Standard is to ensure that offshore structures in arctic and cold regions provide an appropriate level of reliability with respect to personnel safety, environmental protection and asset value to the owner, to the industry and to society in general. [23]

2.1.1. Actions and action effects

The actions and action effects necessary to consider for design depend on the physical environment into which the structure will be placed, as well as the reliability expected of the structure. [23]

The design of arctic offshore structures shall include considerations of global actions, relating to the overall integrity of the structure, foundation and station keeping system, and local ice actions for specific components or portions of the structure. [23]

The actions used for design shall consider all phases of the design service life, including construction, transportation, installation and removal. Allowance for possible weight increase and shift in the center of gravity due to ice accretion during fitting out (if performed in arctic or cold regions) and transportation shall be considered. The allowance shall reflect the time of year and geographical area. Differential strains or lock-in stresses due to temperature changes between construction and permanent locations shall be considered in the design. [23]

2.1.2. Ice actions

2.1.2.1 General principles for calculating ice actions

Direct ice actions and actions arising from the interaction between the ice and the structure shall be considered for both global and local considerations. Such actions can include:

a) static, quasi-static, cyclic and dynamic actions;

b) cyclic and dynamic actions that can cause structural fatigue, liquefaction and personnel discomfort;

c) spatial actions such as rubbling, pile-up, ride-up and similar ice behavior that can hinder operations.[23]

The magnitude of global ice actions and their point of action shall be determined in accordance with specific calculations so that the required integrity of the structure can be assessed. This includes resistance to sliding and overturning, capacity of the foundation, fatigue and foundation liquefaction.

Methods based on full-scale action and response data from measurements on instrumented structures shall be used for the determination of design ice actions on

offshore structures, with due account of their applicability, and for the uncertainties in the data and the methods used in their interpretation. Where no data are available at the location of interest, measurements from other regions may be extrapolated using knowledge of the ice regimes, metocean aspects, climate, brine volume and strength parameters. Small-scale ice strength data obtained locally, preferably *in situ*, can be of assistance in the extrapolation. Physically based models and scale model tests may also be used to complement the full-scale data, with due account for uncertainties in their application.[23]

2.1.2.2. Global ice actions

The determination of global ice actions shall be based on methods that incorporate relevant full-scale measurements, model experiments if they can be scaled reliably, or theoretical methods (analytical or numerical) that have been calibrated using experiments or full-scale measurements. Each of the following conditions shall be considered, and the governing ones shall be used to determine ice actions:

a) quasi-static actions due to level ice (first-year, rafted or multi-year), where inertial action effects within the structure can be neglected;

b) dynamic actions due to level ice (first-year, rafted or multi-year), where inertial action effects within the structure are influential and a dynamic analysis is required;

c) quasi-static actions due to ice rubble and ridges, where inertial action effects within the structure can be neglected;

d) impacts from discrete features such as icebergs, ice islands and large multi-year or first-year ice features;

e) quasi-static actions from features lodged against the structure, driven by the surrounding ice or directly by metocean actions;

f) adfreeze action effects, including the frozen-in condition; and

g) thermal action effects;[23]

The following limiting mechanisms shall be considered.

− Limit stress, which is the mechanism that occurs when there is sufficient energy or driving force to envelop the structure and generate ice actions across its total width. Limit stress actions include direct ice failure against the structure, ice failure within rubble lodged against the structure, floe buckling or floe splitting.[23]

− Limit energy, which is the mechanism that occurs when the interaction is limited by the kinetic energy of the ice feature and is generally characterized by the absence of surrounding ice. Such actions are likely to arise due to impacts of icebergs, refloated stamukhi, multi-year floes or ice islands.[23]

− Limit force, which is the mechanism that occurs when the interacting feature is driven by metocean actions against the structure, and the actions are insufficient for the ice to fail locally and envelop the structure. Such actions are likely to arise where large ice features interact with a structure under the action of wind, current or pack ice pressures, or a combination of these actions.[23]

Ice crushing, shear, flexure, splitting and buckling failure modes should be considered in the calculation of global actions for each of the above failure mechanisms. Where relevant for the scenario, ice conditions and limiting mechanisms, the following factors shall be considered in determining ice actions:

− event frequency;
− geometry of the ice or ice features;
− geometry of the structure;
− mass and added mass of the ice feature;
− mechanical properties of the ice or ice feature;
− ad freeze bond between ice and the structure;
− inertial effects (and added inertia) for both the ice and the structure;
− velocity and direction of movement of the ice features;

− pressured ice conditions;

− ice rubble build-up, and implications for encroachment, structure freeboard requirements and actions transmitted to the structure;

− clearing of ice around the structure;

− ice jamming between the members of a multi-leg structure;

− compliance and damping of the structure and station keeping system;

− dynamic and hydrodynamic effects;

− degree of contact between the ice and the structure;

− friction between the ice and the structure;

− thermal effects in the ice;

− environmental actions of wind, current and pack ice pressure available to drive the ice and their persistence;

− surface morphology and the presence of snow on the ice;

− influence of shoals and other barriers.[23]

2.1.2.3. Ice types - Stage of development

Ice types can be characterized as first-year, second-year, and multi-year sea ice, shelf ice and glacial ice. The term "multi-year ice" is sometimes used to include second-year ice.[23]

The surface appearance of first-year sea ice changes as the ice gets thicker going from black-grey for new and young ice to white when thicker. The stages of development of first-year ice are categorized by the World Meteorological Organization as follows:

a) new (<1 cm thick): sea ice found in small platelets or lumps, usually subdivided into frazil, grease ice, slush or shuga;

b) nilas (1 cm to 10 cm thick): a thin crust of floating ice that easily bends with the waves and swells and has a matt surface appearance;

c) young ice (10 cm to 30 cm thick), subdivided into
−grey (10 cm to 15 cm thick), which often breaks under wave action,
−grey-white (15 cm to 30 cm thick);

d)   thin first-year ice (30 cm to 70 cm thick), is separated into

         −stage 1 (30 cm to 50 cm thick),

         −stage 2 (50 cm to 70 cm thick);

e)   medium first-year ice (70 cm to 120 cm thick);

f)   thick first-year ice (>120 cm thick).[23]

2.1.3. Ice action scenarios

Ice actions are the result of interactions between various ice features and the structure. The shape and size of the structure, the ice conditions and the environmental driving actions can result in a number of different interaction scenarios, failure modes and resulting ice actions. The relationships among the factors that influence the scenarios are illustrated in Figure 10.[23]
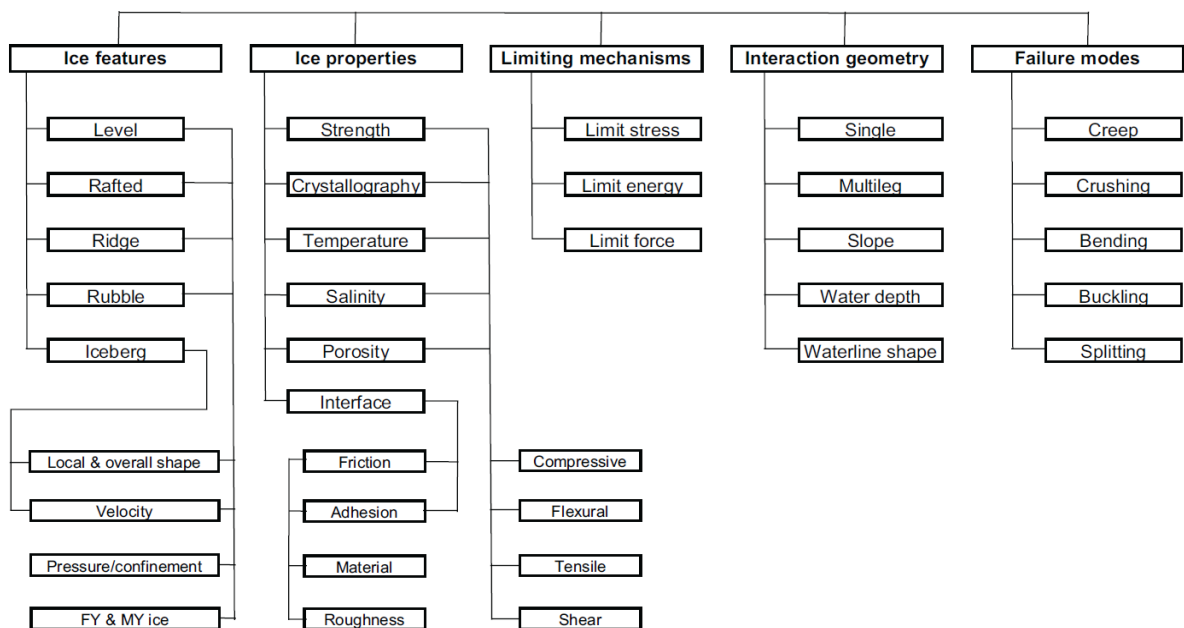
Figure 10. Factors influencing interaction scenarios. [23]

2.1.4. Ice failure modes

2.1.4.1. Overview of failure modes

The mode of ice failure against the structure has a significant effect on the magnitude of the ice action. The failure mode for sea ice (e.g. crushing, shear, flexure, creep) depends on parameters such as ice thickness, presence of ridges, ice

velocity, ice temperature and structure shape. Conditions that induce ice failure by flexure generally result in smaller ice actions than for crushing. Different modes of ice failure can occur on the same structure type depending on ice conditions and interaction velocity, even during the same event. Dynamic structural response is generally associated with ice crushing failure. [23]

Structure geometry is an important factor in determining ice actions. Key design features include the structure type (multi-leg, monopod or caisson), vertical or sloping waterline geometry (see Figure 11), the plan shape of the structure and the plan dimensions. Braces or appendages should not be exposed to ice actions. [23]
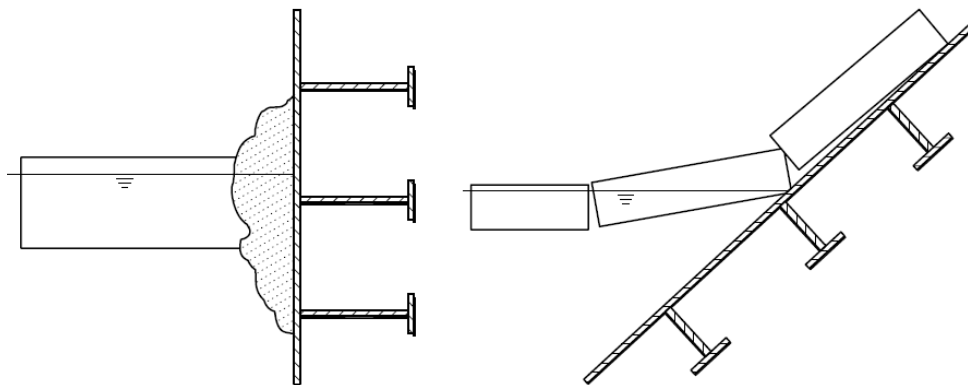
a) Crushing failure (vertical structure) b) Bending failure (sloping structure)

Figure 11. Failure modes. [23]

The profile of the structure is a key issue. Structures with vertical walls in the waterline region generally experience larger ice actions than sloping ones for similar waterline dimensions. Ice actions are generally less for sloping structures, except in situations where large amounts of ice rubble accumulate on the sloping surface. If this occurs, flexural failure can be impeded and different modes or mixed modes of failure can occur with potentially larger actions.[23]

The plan shape of a structure is less important, except in situations where a corner of a rectangular structure is oriented towards the preferred ice motion

direction. Generally, the waterplane form of a structure has a 10 % to 15 % influence on the magnitude of global ice actions.[23]

The plan dimensions of the structure influence the magnitude of ice actions. Many experiments and observations demonstrate the existence of a size effect, whereby the global or effective pressure (total action divided by the nominal contact area) for a narrow structure is higher than for a wide one.[23]

Break-out of an ice feature frozen around a structure can potentially generate large ice actions. Such behavior is more likely in areas of very small tidal range. While experience has shown that this situation is not generally critical for the design of large offshore structures, the issue should be addressed.[23]

a) Ice sheet interaction with the flat surface of a narrow vertical structure

b) Profile of ice sheet interaction with vertical structure
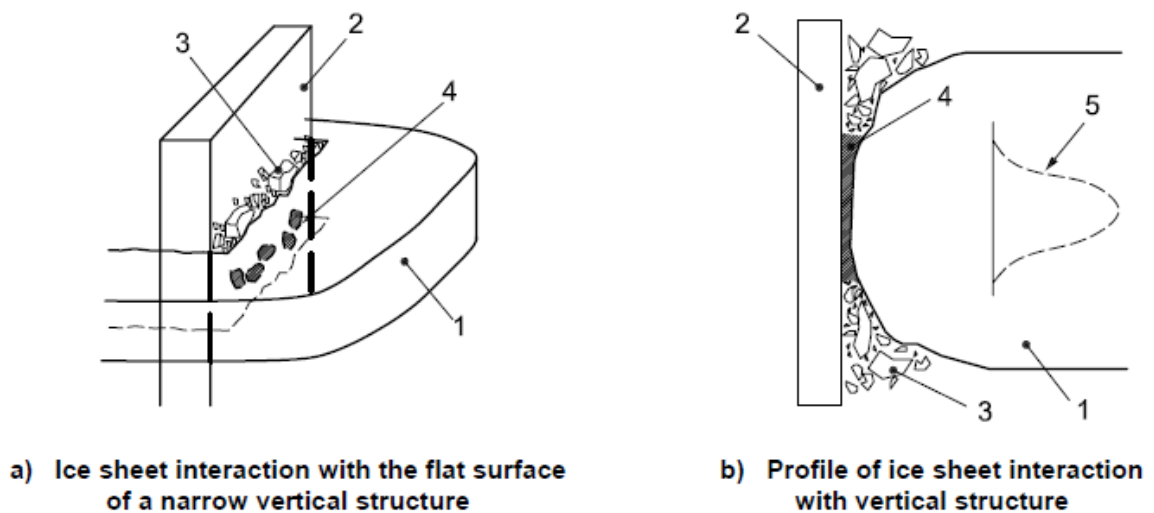
Key

1 ice sheet

2 structure

3 spalls and extrusion

4 high pressure zones in a), layer of crushed ice of high pressure zone in b)

5 pressure distribution over the contact surface. [23]

Figure 12. Schematic showing localization of actions. [23]

2.1.5. Vertical structures – Global pressure for sea ice

Data obtained from full-scale measurements in Cook Inlet, the Beaufort Sea, Baltic Sea and Bohai Sea have been used to determine upper bound ice pressure values for scenarios where a first-year or multi-year ice acts against a vertical structure. The data have also been used to analyze how the ice thickness and the width of the structure influence the global ice action. Based on these studies, the global ice pressure can be determined as given in Equation (1):

$$p_G = C_R * \left(\frac{h}{h_1}\right)^n * \left(\frac{w}{h}\right)^m \tag{1}$$

where

p_G is the global average ice pressure, expressed in megapascals;

w is the projected width of the structure, expressed in metres;

h is the thickness of the ice sheet, expressed in metres;

h_1 is a reference thickness of 1 m;

m is an empirical coefficient equal to -0,16;

n is an empirical coefficient, equal to -0,50 + $h/5$ for h <1,0 m and to -0,30 for h >1;

C_R is the ice strength coefficient, expressed in megapascals.[23] C_R= 2.5 to 2.8 for level ice in cold areas.

2.1.6. Sloping structures - Description of the failure process

Offshore structures with a sloping surface can be considered as an alternative to a vertical structure. Level ice interacting with a sloping structure is more likely to fail in a flexural failure mode. Ice actions in such failure modes can be significantly lower than in a crushing failure mode, which is typical for vertical-sided structures. Sloping icebreaking surfaces can also reduce ice actions from ice ridges. [23]

A side geometry that is formed of two sloping flat surfaces can be used in areas where the ice movement has a dominant direction. Studies have also been

done on sloping flat panels to obtain fundamental understanding of the ice actions due to sheet ice. Flat sloping panels can also be used as a part of a structure. [23]

Sloping structures break the oncoming sheet ice by deflecting it either upwards or downwards. The resulting ice action has both a vertical and horizontal component. The horizontal and vertical components of ice action on a downward breaking structure are lower relative to those acting on an upward breaking structure of the same size and slope angle. In the case of a downward breaking structure, the vertical component of the ice action is directed upwards, reducing the effective shear resistance at the structure-seabed interface. [23]

Ice interaction with a sloping surface is a complicated process that includes failure of intact ice, ride-up of broken ice pieces, accumulation of ice rubble on the slope, and subsequent clearing of the rubble accumulation; see Figures 13. [23]

a) Ice sheet approaches structure
b) Ice begins to fail and ride up face of structure
c) Ice blocks ride up face of structure and are turned back at vertical face
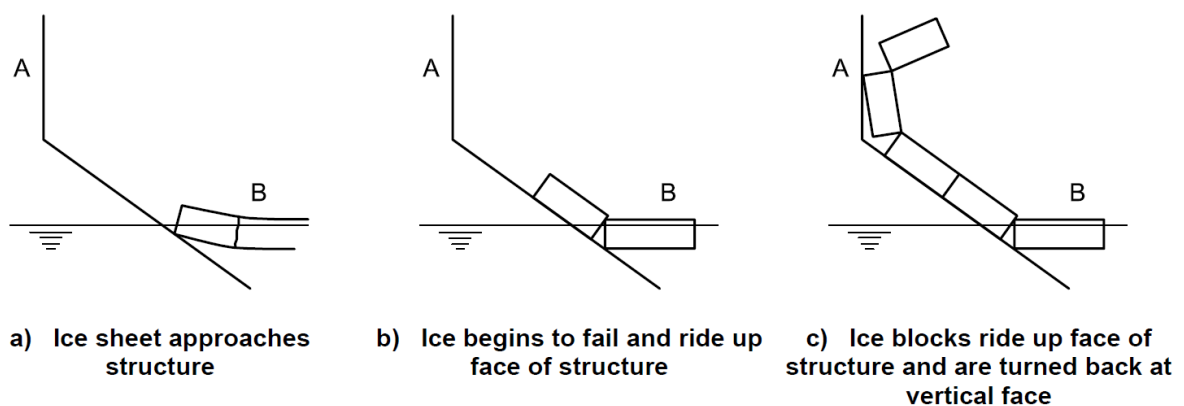
Figure 13. Processes in the interaction between a sloping structure. [23]

Key

A - sloping structure; B - encroaching ice sheet

Ice rubble can also accumulate under the ice sheet, further complicating the interaction process. The maximum ice action on a sloping structure is hence a function of several different parameters including bending, compressive and shear

strengths of the ice sheet, friction coefficient between structure surface and ice, presence of snow, density of ice, and the height and geometry of ice rubble.[23]

Figure 14 depicts level ice action components for a two-dimensional interaction with an upward breaking structure. The horizontal and vertical components of ice action are as given by Equations (2, 2.1):

$$F_h = Nsin\alpha + \mu Ncos\alpha \qquad\qquad (2)$$

$$F_v = Ncos\alpha + \mu Nsin\alpha \qquad\qquad (2.1)$$

where

N is the component normal to the structure surface;

α is the inclination angle of the structure surface from the horizontal, expressed in radians;

μ is the coefficient of kinetic friction between the ice and structure surface. [23]

The relationship between the vertical and horizontal components is given by Equation (3)

$$F_v = \frac{F_h}{\varepsilon} \qquad\qquad (3)$$

where

$$\varepsilon = \frac{sin\alpha + \mu cos\alpha}{cos\alpha - \mu sin\alpha} \qquad\qquad (3.1)$$

Theoretical models developed to calculate level ice actions on sloping structures can provide reasonably accurate estimates of ice action, as long as the input data and assumptions are appropriate.[23]

A number of methods of determining ice actions on cones and sloping structures have been developed, two of which are described below. The first is based on the theory of plasticity, and the second is based on elastic beam bending.[23]

Besides the parameters used in Equations (2, 2.1) and (3), the following parameters are used in the two models, with the various parameters expressed in consistent units:

H_B is the horizontal action on the cone due to ice breaking;

V_B is the vertical action on the cone due to ice breaking;

H_R c;

V_R is the vertical action on cone due to ride-up;

σ_f is the flexural strength of the ice sheet;

h is the thickness of the ice sheet;

w is the waterline diameter of the cone or width of a sloping structure;

ρ_i is the density of ice;

ρ_w is the density of water;

g is the acceleration due to gravity;

ν is the Poisson ratio for ice, typically equal to 0,3.[23]
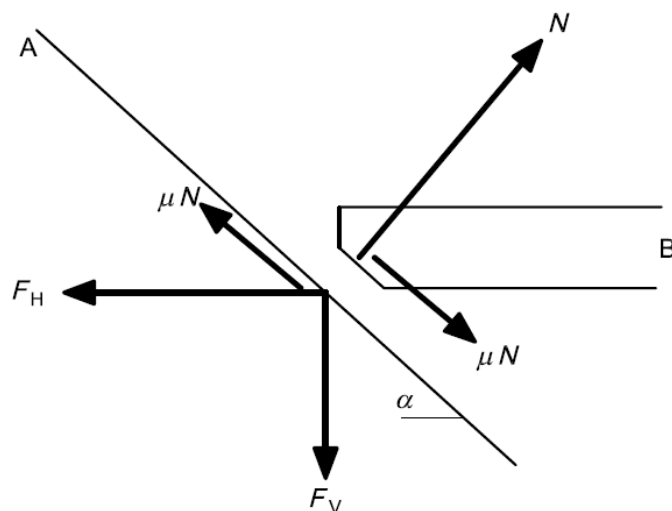
Key

A   sloping face of structure;

B   encroaching ice sheet;

N normal component of reaction to ice action on structure;

μ   ice-structure friction coefficient;

α   slope of structure face from horizontal;

F_H horizontal component of ice action;

F_V vertical component of ice action.

Figure 14. Ice action components on a sloping structure for a two-dimensional condition.
[23]

2.1.7. Plastic method for cones

This method is based on a limit analysis solution for level ice actions on upward and downward breaking cones. The model considers actions due to the flexural failure of the ice sheet and the ride-up actions due to ice pieces. The derivation is for an upward breaking cone and is also valid for a downward breaking cone if ρi is replaced with $(\rho_w - \rho_i)$.The functions as given by Equations (4) to (7) are defined for the solution:[23]

$$f = sin\alpha + \mu E_1 cos\alpha \tag{4}$$

$$g_r = \frac{sin\alpha + \frac{\alpha}{cos_\alpha}}{\frac{\pi}{2}sin^2\alpha + 2\mu\alpha cos\alpha} \tag{5}$$

$$h_v = \frac{fcos\alpha - \mu E_2}{\frac{\pi}{4}sin^2\alpha + \mu\alpha cos\alpha} \tag{6}$$

$$W = \rho_i gh_r \frac{w^2 - w_T^2}{4cos\alpha} \tag{7}$$

where

α   is the slope of the structure measured from the horizontal, expressed in radians;

w_T is the top diameter of the cone;

h_r is the ice ride-up thickness ($h_r \geq h$).[23]

The effects of a rubble accumulation on the cone can be considered by using a value that exceeds the single sheet thickness for the ride-up thickness. The parameters E_1 and E_2 are the complete elliptical integrals of the first and second kind, defined as given by Equations (8 and 9):

$$E_1 = \int_0^{\pi/2} (1 - sin^2\alpha sin^2\tau)^{-1/2} d\tau \tag{8}$$

$$E_2 = \int_0^{\pi/2} (1 - sin^2\alpha sin^2\tau)^{1/2} d\tau \tag{9}$$

Assuming a single sheet thickness of ride-up ice, the horizontal ride-up action, H_R, and the vertical ride-up action, V_R, are obtained as given by Equations (10,11) [23]

$$H_R = W \frac{tan\alpha + \mu E_2 - \mu f g_r cos\alpha}{1 - \mu g_r} \tag{10}$$

$$V_R = W cos\alpha \left(\frac{\pi}{2} cos\alpha - \mu\alpha - fh_v \right) + H_R h_v \tag{11}$$

The horizontal breaking action H_B and the vertical breaking action V_B are given by Equations (12) and (13) [23]:

$$H_B = \frac{\sigma_f h^2}{3} \frac{tan\alpha}{1 - \mu g_r} \left[\frac{1 + Yxlnx}{x - 1} + G(x - 1)(x + 2) \right] \tag{12}$$

$$V_B = H_B h_v \qquad (13)$$

Where

Y is equal to 2,711 for Tresca yielding or equal to 3,422 for Johansen yielding;

G is equal to $(\rho_I g w^2)/(4\sigma_f h)$;

X is given by Equation (14): [23]

$$x = 1 + (3G + \frac{Y}{2})^{-1/2} \qquad (14)$$

The total action components in the horizontal and vertical directions are given, respectively, by Equations (15) and (16) [23]:

$$F_H = H_B + H_R \qquad (15)$$

$$F_V = V_B + V_R \qquad (16)$$

2.2. Overview of the CAN/CSA-S471-04

CAN/CSA-S471-04 - General requirements, design criteria, the environment, and loads.

This Standard specifies minimum requirements for and provides guidance on design principles, safety levels, and loads in connection with the design, construction, transportation, installation, and decommissioning of offshore structures.[24]

Ice loads depend on geographical location, season, ice feature type, interaction scenario, and structural configuration. With these considerations taken into account, a structure shall be designed for rare environmental events or events associated with frequent environmental processes, which can include: [24]

(a) iceberg impacts;

(b) interactions with sea ice, whether first-year or multi-year, and whether level, deformed, or ridged;

(c) interactions with ice islands or fragments thereof.[24]

Design loads shall generally be calculated from event frequencies and associated load magnitudes using a probabilistic approach and accounting for appropriate distributions of ice and related parameters. [24]

For preliminary analysis (e.g., concept selection), deterministic ice load calculations based on 100-yearice events may be used in the context of sound engineering judgment. [24]

Loads shall be calculated for the structure as a whole to ensure overall stability, and for local contact areas to ensure structural integrity. The structure shall have the inherent strength to withstand safely, though not necessarily without local damage, the design ice loading.[24]

Although ice loads have generally been treated as equivalent static loads, their amplitude, frequency, and duration content are important and shall be considered.[24]
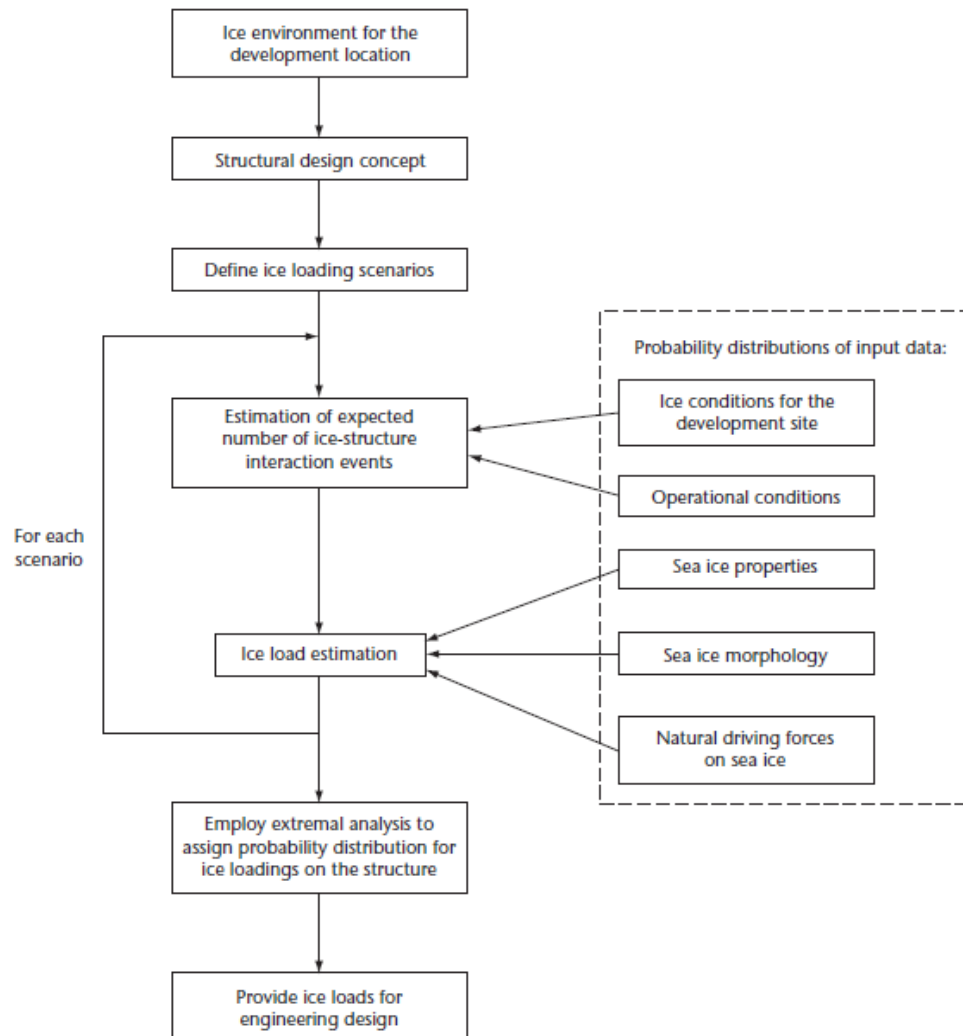
Figure 15. A general framework for the probabilistic approach. [24]

2.2.1. Ice load scenarios

The ice load scenarios to be considered depend on the geographical location and must be specified in such a way as to include an adequate description of hazards for the site under consideration. The scenarios fit into the overall framework of the analysis as illustrated in Figure 14and form the basis for probabilistic modelling. [24]

When applicable, the scenarios to be considered shall include interaction with:

(a) first-year ice features (level ice, rafted ice, landfast ice, floes, ridges, rubble fields);

(b) multi-year ice features (level ice, floes, ridges, rubble fields);

(c) icebergs;

(d) ice islands (ice shelf fragments).[24]

Subsidiary conditions relating to the scenarios described above can include:

(a) seasonality;

(b) ocean currents;

(c) wind;

(d) waves;

(e) operational criteria (detection, shutdown, physical management, disconnection).

These can act in combination with the ice features or influence the nature of the interaction. [24]

2.2.2. Considerations for load calculations

The value of the load at a specified probability of exceedance depends on many parameters, a number of which are uncertain and require probabilistic treatment. The following shall be considered, where appropriate:

(a) the event frequency;

(b) the geometry and mass of the ice features;

(c) the velocity of the ice features;

(d) the eccentricity of the collision;

(e) the point of action of the load;

(f) the added mass of ice and structure;

(g) the presence of surrounding pack ice;

(h) ice rubble build-up before and during the events;

(i) the compliance of the structure;

(j) relevant ice properties for individual events, including measures of ice strength.[24]

Many of these parameters depend on geographical location and season.

A key element in the specification of event parameters is that they represent the population for those ice features impacting the structure. Specifically, distributions for parameters such as ice feature size and velocity shall be corrected to reflect the fact that larger or faster ice features are more likely to impact the structure.[24]

2.2.3. Ice load mechanisms

There are three basic mechanisms by which ice loads can be exerted on a structure:

(a) limit stress: the maximum load for an event is governed by the failure of the ice immediately adjacent to the structure;

(b) limit energy: the maximum load for an event is limited by the kinetic energy of the impacting feature;

(c) limit force: the maximum load for an event is limited by force applied by or to the ice feature (this can include gravity).[24]

2.2.4. Ice pressures for global load estimation - Contributing factors

For calculating global loads, the ice pressure may depend on
    (a) the geometry of the structure;
    (b) the size of the nominal contact area;
    (c) the aspect ratio (the ratio of width to height, W/h, of the nominal contact area);
    (d) the speed of the interaction;
    (e) the composition of the ice (floe size and variability in thickness);
    (f) the ice temperature and porosity.[24]

The nominal contact area is the projected area of the intact ice feature on the structure, which can change during an ice-loading event as the structure penetrates the ice. For massive ice features such as icebergs, the nominal contact area is the area of ice that would be in contact with the structure had the ice feature

maintained its original shape during the course of the interaction. For sea ice features, the nominal contact area is typically. [24]

$$A = Wh \tag{17}$$

where

W = the contact width against the structure

h = the thickness of the ice feature

The global average pressure decreases with increasing nominal contact area. As a result, pressure-area relationships are used to model the pressures over nominal areas. Global loads can be calculated using either a random pressure-area relationship capturing the variability of the average global pressure or a constant pressure selected to achieve appropriate safety.[24]

2.2.5. Ice forces on structures with vertical faces - Basic strategy

Subject to the kinetic energy and driving force limitations, ice forces on vertically faced structures are governed by the deformation and failure of the ice adjacent to the face of the structure. For vertical structures, the ice failure process can include crushing, clearing, spalling, and other fracture mechanisms.[24]

The current state of practice is not to model all of these processes explicitly, but to calculate ice forces from the expression

$$F = PA \tag{18}$$

where

F the ice force at a specified stage in the interaction

P the corresponding average ice pressure on the contact face over the nominal contact area A. [24]

The specification of ice pressure is outlined in above. The nominal contact area is the projected area of the intact ice feature on the structure (i.e., at the penetration corresponding to the design load).[24]

This contact area can exceed the actual loaded area of the structure at any time. The nominal contact area can depend on

(a) the shape of the structure; and

(b) the local shape of the ice feature.

The ice force corresponding to a loading event will be the maximum value of F over the course of the interaction. Both P and A should be treated as random quantities. [24]

2.2.6. Ice forces on structures with sloping faces - General

Sloping structures can be narrow or wide, upward breaking or downward breaking. The general approach to predicting sheet ice loads on a conical or sloping structure is described in Croasdale work. [29] The design load will be the sum of the ice-breaking and ice-clearing forces. The ice-breaking forces are determined from the failure of a plate on an elastic foundation using either an elastic brittle or a plasticity approach, the latter approach being rather conservative. An important parameter is the large-scale flexural strength of the ice. The ice-clearing forces depend on buoyancy, gravity, rotation, friction, and inertia effects. The interaction of advancing ice blocks with the superstructure or the neck of a conical structure may also be considered.[24]

2.2.7. Sloping structures — Sheet ice

In 1980 Ralston [27] developed a plastic-limit analysis for ice failure on a cone. In 1992 Nevel [28] derived a method based on elastic theory with ice segments formed on the cone surface. Croasdale developed a theory based on a two-dimensional analysis of the failure and ride-up of a floating ice plate.[29] This approach resulted in a relatively tractable equation in which the first term can be considered to be the force to break the ice, and the second term the force due to ice riding up the slope of the structure.

In the three-dimensional situation, when the ice is wider than the structure, it can be intuitively appreciated that the failure zone will extend to a greater width than the structure. In this situation, the ice-breaking term will be greater than the two-dimensional analysis indicates. A simple correction of the two-dimensional analysis to account for this effect was suggested by Croasdale. [29]In these theories, there is always uncertainty regarding the amount of ice pile-up on the structure. This can add appreciably to the load and can alter the failure mode of the underlying ice sheet.

Although there have been a very large number of physical model tests of ice loads on sloping structures, no comprehensive compilation is available.[24]

2.3. Overview of SNIP-2.06.04-82

SNIP-2.06.04-82 - Loads and Impact Ice on Hydraulic Structures

Load of ice on hydraulic structures caused by limiting ice breaking force should be determined based on initial data of ice conditions in the area of structures for a period of time with the greatest ice impact.[25]

Normative ice resistances in compression R_c, MPa, bending R_f, MPa, and collapse R_b, MPa, shall be determined from experimental data, and in their absence is allowed:

a) to take R_c from Table. 2

Table 2. Table for determining the coefficient R_c. [25]

Ice salinity S_i, %	Normative ice compression resistance R_c, MPa, with an average daily air temperature t_a, °C			
	0	-3	-15	-30
Less than 1 (fresh waterice)	0,45	0,75	1,2	1,5
1 - 2	0,4	0,65	1,05	1,35
3 - 6	0,3	0,5	0,85	1,05

t_a, °C - average temperature three-day period prior to the action on the ice structure in ice thickness of 0.5 m or less, or for a six-day period when ice thickness greater than 0.5 m;

S_i, % - salinity of the ice, to be considered equal to 20% of salinity ice age up to two months or 15% salinity - ice age two months or more.

b) to determine the R_f by the formulas:

for freshwater ice

$$R_f = 0,75R_c \tag{19}$$

for sea ice

$$R_f = 0,5R_c \tag{20}$$

c) to determine R_b, according to the formula

$$R_f = k_b R_c \tag{21}$$

where k_b - coefficient taken from Table. 3

Table 3. Table for determining the coefficient k_b. [25]

Value b/h_d	1	3	10	20	30 and more
Coefficient k_b	2,5	2	1,5	1,2	1

b   width of structures on the front and at the action of ice, m;

h_d estimated ice thickness, m.

2.3.1. Loads from ice fields on hydrodynamic structures

Force caused by moving of ice floes acting on hydrodynamic structures with a vertical wall should be determined:

1) from the effects of the ice field on a freestanding beam with the front edge of a triangular outline while cutting her by ice $F_{b,\,p}$, MN, or when the ice field is stopped by support beam $F_{c,p}$, MN, for the smaller value defined by the formulas:[25]

$$F_{b,p} = mR_b b h_d \tag{22}$$

$$F_{c,p} = 0,04vh_d\sqrt{mAR_b tg\alpha} \tag{23}$$

2) from the effects of moving ice floes onto freestanding support beams with any contours while cutting them by the ice Fb, p, MN, by the formula (22);

3) from the effects of moving ice floes on extended structures ($b/h_d \geq 50$) impacted by individual floes $F_{c,\,w}$, MN, or the crushing of ice $F_{b,\,w}$, MN, determined by the formulas 24 and 25:[25]

$$F_{c,w} = 0,07vh_d\sqrt{AR_c} \tag{24}$$

$$F_{b,w} = 0,5R_c b h_d \tag{25}$$

where

m   the form factor in terms of support beam, defined by Table. 4;

v   velocity of the ice floe, m/s, which is determined according to field observations, and in their absence it is allowed to take it equal to: for the rivers and tidal areas of the seas - the speed of the water flow; for reservoirs and seas - 3% of the wind velocity with 1% frequency of exceedance during the period of the action of the ice;

A   area of the ice field, m^2, determined by field observations in this or related areas;

α   inclination of the wall, degrees

Table 4. Table for determining the coefficient m. [25]

Shape coefficient	For support beams in forms						
	Triangle with inclination angle, degree					Rectangular	Polyhedron or semicircular contours
	45	60	75	90	120		
m	0,54	0,59	0,64	0,69	0,77	1	0,9

To find the force from the impact of the ice floes on structures with sloping profile or on a freestanding support beam's inclined surface, it is necessary to determine:

1. the construction of the sloping profile:

a) a horizontal component of force F_h, MN - the lowest values which are obtained by the formula (26) and the formula (22)

$$F_h = k_b m_t R_f h_d^2 \tag{26}$$

b) a vertical force component F_v, MN, - given by the formula

$$F_v = \frac{F_h}{m_t} \tag{27}$$

2. on a freestanding support beam with a sloping front edge;

    a) a horizontal component force $F_{h, p}$, MN - the lowest value obtained by the formulas (22) and (26);

    b) a vertical force component $F_{v, p}$, MN, - of formula (27) *;

    where k_β - coefficient taken from Table 5;

    m_t - the coefficient taken from Table 6;

    R_f, h_d, b - the notation is the same as above; [25]

<p align="center">Table 5. Table for determining the coefficient k_β. [25]</p>

Type of obstacles or structures	Prop rectangular cross section value of b/h_d		Conical prop	Construction of slope profile
	5 and below	5 and above		
Coefficient k_β	1	$\dfrac{0,2b}{h_d}$	$1 + \dfrac{0,05b}{h_d}$	$0,1b$

<p align="center">Table 6. Table for determining the coefficient m_t. [25]</p>

Angle of wall inclination β, degree	15	30	45	60	75	80	85
Coefficient m_t,	0,27	0,58	1	1,73	3,73	5,67	11,43

    Force caused by moving of ice fields F_p, MN, on the support structures of a series of vertical poles located at distance l, m, for values b/l from 0.1 to 0.9 should be taken as the smallest of the values defined by the formulas (22) and (23)*, and the formula[25]:

$$F_p = \left[\frac{b}{t} - (1 - 2mk_b) + 2mk_b\right] F_{b,w} \tag{28}$$

2.4. Overview of the VSN 41.88.
VSN 41.88 - Loads and effects of ice

These rules consider the maximum load and the impact of ice on support beams of structures erected on the shelf in freezing seas, at speeds of progress of the ice fields up to 0.5 m/s. Load from ice fields of finite size in the open sea, with the drift velocity over 0.5 m/s is to be determined in accordance with the recommendations of SNIP 2.06.04-82.[26]

The normative value of ice load is determined based on:

1) statistical data on hydrological and ice regime of the area of construction
(daily average air temperature, salinity of water and ice, the nature of fluctuating water levels, ice thickness, it's hummocking, character and the movements (drift) of the ice fields);

2) physical and mechanical properties of ice ;

3) Geometric parameters data of support beams and the conditions of contact with the ice.[26]

The main strength characteristics which are determining the size of the ice load on the structure include:

a) regulatory resistance R_c ice compression, MPa;

b) regulatory ice bending resistance R_f, MPa.[26]

Normative values for R_c, R_f are accepted average values of the experimental data test samples on ice strength.[26]

In the absence of such data is allowed to take regulatory ice bending and compression resistances from tables 7 and 8 respectively. [26]

<p style="text-align: center;">**Table 7. Table for determining the coefficient R$_c$. [26]**</p>

Icesalinity S, %	Normative ice compression resistance Rc, MPa, with an average daily air temperature t_a, °C			
	- 2°	- 10°	- 20°	- 30°
1 and less	1,00	1,40	1,50	1,55
2	0,75	1,25	1,35	1,45
3	0,60	1,15	1,30	1,40
4	0,40	1,10	1,25	1,30
5	0,30	1,00	1,20	1,25
6	0,20	0,95	1,15	1,20

<p style="text-align: center;">**Table 8. Table for determining the coefficient R$_f$. [26]**</p>

Icesalinity S, %	Normative ice bending resistance Rf, MPa, with an average daily air temperature t_a, °C			
	- 2°	- 10°	- 20°	- 30°
1 andless	0,50	0,60	0,65	0,70
2	0,40	0,55	0,60	0,65
3	0,30	0,50	0,55	0,60
4	0,25	0,45	0,50	0,55
5	0,20	0,40	0,45	0,50
6	0,15	0,35	0,40	0,45

Where

t_a the average temperature for the coldest six-days period in a year on a 5 year series of observations;

S   salinity of the ice was assumed to be 15% salinity of ice age 2 months or more.

Support beams with a natural frequency of 2 Hz should be calculated as absolutely rigid structures during the following types of actions:

a) the impact of flat and hummocky ice fields at their horizontal movement

b) the impact of ice cover on frozen construction due to fluctuations in water level.[26]

Point of application of the resultant ice loads must be taken below the calculated water level at 0,3 h.[26]

Horizontal load on a freestanding pole with a vertical surface during progress of the ice field should be defined as:

$$F_{b,p} = m_1 K_b R_c b h_d \, , MN \qquad (29)$$

Where

m_1 coefficient taking into account the form of the support beam, it's equal to: for round and polygonal towers - 1.0 and for rectangular towers - 1.1;

b   transverse dimension along the front of support beam on the level of action of ice, m;[26]

<div align="center">

Table 9. Table for determining the coefficient K_b. [26]

</div>

Value	b/h_d	1	2	4	6	7	10	12	16	20	30 and more
Buckling coefficient K_b	Without freezing of support beams by ice field	6,0	4,5	2,9	2,2	1,8	1,6	1,4	1,2	1,1	1,0
	With freezing of support beams by ice field	6,0	5,0	3,7	3,1	2,8	2,7	2,6	2,5	2,3	2,2

The total horizontal load on the structure, consisting of a system of vertical pillars, with progress of the ice field to be determined by the formula 30:[26]

$$F_n = n K_1 K_2 F_{b,p} \, , MN \qquad (30)$$

where

n   total number of supporting columns in construction;

$F_{b,p}$ horizontal load on a freestanding supporting column, defined by the formula (29);

K_1 coefficient of "heterogeneity" of the ice, defined by the formula (31): [26]

$$K_1 = \frac{1 + \xi n^{-1/2}}{1 + \xi} \tag{31}$$

where

ξ coefficient of variation of the strength of ice samples for uniaxial compression (R_c) in the absence of field data is allowed to take value $\xi = 0,2$;

K_2 the coefficient of "interference" equal:

If $b/l \geq 1$, then $K_2 = K_b (n)/K_b$;

if $0,1 < b / l < 1m$ then K_2 is determined by linear interpolation between the values of $K_b (n)/K_b$ and 1;

if $b/l \leq 0,1$, then $K_2 = 1$,

where $K_b (n)$ and K_b − buckling coefficients for the system of support beams for the support beam unit, respectively, values should be determined from Table. 6, wherein:

$K_b (n)$ is determined by ratios $b_f/h_d = n_f b/h_d$;

K_b is defined at the ratio b/h_d,

where

b, h_d designations are the same as in above;

l   distance between the front axle supports, in m;

b_f the total width of the front supporting columns to facilities

$b_f = n_f b,$

where n_f - number of columns on the front of the building.

Vertical ($F_{v.p}$) and horizontal ($F_{h.p}$) components should be determined by the formulas:[26]

$$F_V = K_\alpha R_f h_d^2, MN \qquad (32)$$

$$F_H = F_V tg(\alpha + arctgf), MN \qquad (33)$$

where K_α- coefficient determined from the relationship:[26]

$$K_\alpha = \begin{cases} 3,00 & in & \dfrac{b}{h_d} < 5 \\ 2,75 + 0,05\dfrac{b}{h_d} & in & 5 \leq \dfrac{b}{h_d} \leq 15 \\ 2,00 + 0,10\dfrac{b}{h_d} & in & \dfrac{b}{h_d} > 15 \end{cases} \qquad (34)$$

b   the width (diameter) of the conical support beam, m;

α   angle of the cone to the horizontal surface;

f   the coefficient of friction of ice on the conical surface of the support;[26]

2.5. Overview of API RP 2N

API RP 2N – Recommended Practice for planning, designing, and constructing fixed offshore structures in Ice Environments.

2.5.1. Load consideration

General

All loads expresses in this section are unfactored loads. Depending on the design method that is being used for a particular structure, these loads may need to be modified by an appropriate load factor to represent the design loading properly.[30]

Evaluation of effects from design loadings requires combining various load categories that are expected to act on a structure simultaneously. Considerations on how to combine loads to identify critical effects on the structure and the foundation are given below contains guidelines on ice features expected in several areas of the U.S. continental shelf.[30]

Dead loads.

Dead loads are static loads that may be considered as constant in magnitude and fixed position.[30]

Live Loads.

Live Loads may be static or dynamic in nature. These are generally gravity loads that result from normal operations of the structure. They may vary in magnitude and position. Loads from weight and buoyancy of sea ice that may freeze to the structure in the vicinity of the splash zone should be included as live loads. [30]

In addition to the usual live loads associated with oil production activities, some structures in ice environments may be designed to provide vertical support to well conductors. Well conductors may be subject to downdrag (negative skin factor) loads due to differential settlement of the soil, caused by consolidation or thawing. [30]

Deformation Loads.

Deformation loads are static loads due to deformations imposed on the structure. They are structure dependent and are caused by such phenomena as:

- presteressing forces;
- shrinkage and expansion;
- creep;
- foundation differential settlement.[30]

Accidental Loads.

Accidental loads are generally dynamic loads that result from accidents, misuse, or other exceptional conditions. Accidental loads may result from:

- impact due to dropped objects
- impact caused from collisions with boats, barges, or other craft
- effects of fires or explosions
- sudden loss of pressure in buoyancy chambers, etc.[30]

Environmental Loads.

Environmental loads are static or dynamic loads that are used by natural phenomena, such as:

- Wind;
- Waves;
- Currents;
- Earthquakes;
- Ice;
- Temperature changes.[30]

Construction Loads.

Construction loads are temporary loads, static or dynamic in nature, that fall into all the above load categories, but that assume special importance during construction of a structure. Because the level of structural strength during

construction is variable, the magnitude of loads during construction should be carefully monitored against the available structural and foundation strengths.[30]

Transportation loads.

Transportation loads are temporary loads encountered by the structure during its transport from the construction to the installation sites, and for mobile structures during relocation.[30]

Examples of transportation loads are:

- Loads exerted by tow-lines;
- Loads from waves during tow to the installation site, including inertial forces due to structure motion;
- Impact loads from sea ice when under tow;
- Air pressure underneath the base of a structure;
- Hydrostatic pressure as a result of flooding due to structural damage during transportation. [30]

Installation Loads

Installation loads are temporary loads, static or dynamic in nature, that are associated with the installation activities of a structure or its equipment such as:

- Pile driving;
- Flooding and upending;
- Deck module lifts onto a structure;
- Submergence;
- Mobile structure relocation.[30]

In the case of gravity structures which are ballasted onto the seafloor, the structure should be designed for the anticipated loads during touchdown, skirt penetration, and ballasting.[30]

2.5.1. Determination of ice loads

This paragraph provides considerations on load predictions from ice contact with a structure. The prediction of ice loads on a structure is complicated ice-structure-foundation interaction problem.[30]

Ice loads on structures consist of both global and local loads. Global ice loads represent the total ice loads acting against the structure, while local ice loads represent the magnitude of ice pressure on some area of the structure.[30]

Local and global ice loads magnitudes depend on a number of factors including the following:

- The geometry of the ice feature;
- The physical and mechanical properties of the ice feature;
- The failure mode induced in the feature or in the surrounding ice sheet as a function of the structure geometry;
- The degree and eccentricity of contact between the ice feature and the structure;
- The velocity of the ice feature;
- The environmental forces available to drive the ice feature;
- The inertial effects in both the ice and the structure;
- Friction between the structure and ice;
- Compliance of the structure;
- Non-simultaneous failure of the ice in a given mode;
- Simultaneous occurrence of different failure modes.[30]

Ice loads may be limited by ice feature failure at the ice-structure interface, or by limitations in driving force at locations away from structure. These limitations may result from physical limits to environmental driving forces, or by alternative ice failure modes. For example, the load transmitted by a large multiyear floe to a structure will be lesser of the load to fail the floe at the floe-structure interface or the load transmitted to the floe surrounding ice pack. [30]

Methods for computing ice loads for offshore structures are based on a combination of large and small scale experimental studies, analytical studies, and model test results. Model test have proven useful qualitatively, for example, in evaluating probable ice failure modes.[30]

Quantitative use of model tests must take proper account of differences in material properties between real ice at full scale and real or model or model ice at model scale, as well as other scaling relationship.[30]

Wide structures.

A wide structure is one with a width much larger than the maximum expected ice feature thickness. For wide structures, more than one zone of ice failure may occur across the width of the structure.[30]

One type of wide structure is a man-made island. Island may be constructed of any material, but the usual materials are earth fill or spray ice. The main characteristics of islands are their large size (diameter) and their reliance on gravitational forces to develop foundation resistance against ice loads. Although islands, particularly gravel islands, have sloping sides, loads on islands should be calculated assuming vertical sides because of the nature of ice/structure contact surface.[30]

2.5.2. Loads- limited by ice strength.

Sheet or floe Crushing.

Korzhavin equation. The horizontal force exerted by ice crushing against a structure may be calculated as:

$$F = I f_c C_x D t \qquad (35)$$

In which $I f_c C_x$ is the average ice pressure and $D t$ is exposed area of the structure, and where:

F   horizontal ice force;

I   indentation factor;

F_c contact factor;

C_x unconfined compressive strength of the ice;

D   diameter or width of the structure at the region of ice contact;

T   ice thickness.[30]

(a) Ice velocity effects. The strain rate based on the instantaneous velocity the ice cover and can be defined for conditions of breakout and continuous crushing.

The strain rate associated with the initial crushing failure of ice frozen against a structure may be associated with the buildup of driving forces, resulting largely from storm winds. Breakout occurs when the ice, initially at rest, starts to move. The condition of continuous crushing occurs following breakout, and the ice velocity cam be estimated from horizontal site specific ice movement.[30]

(b) Indentation Factor. The indentation factor, I, which is ratio of ice crushing pressure to ice unconfined compressive strength as used in Equation 35, depends on:

- Crystallographic structure of the ice;
- Geometry of the interaction between the ice and the structure;
- Definition of strain rate.[30]

Figure 15 gives an example of indentation factors for laboratory grown columnar fresh water ice, which has a high degree of strength anisotropy. The curves in this figure tend toward an indentation factor of 3.0 for large aspect rations. These have been used for columnar saline ice. [30]

(c) Contact factor.

The contact factor, f_c, is empirical and depends on:
- Ice movement rate;
- Local geometric effects;
- Ice crushing mechanism;
- Size effect.[30]
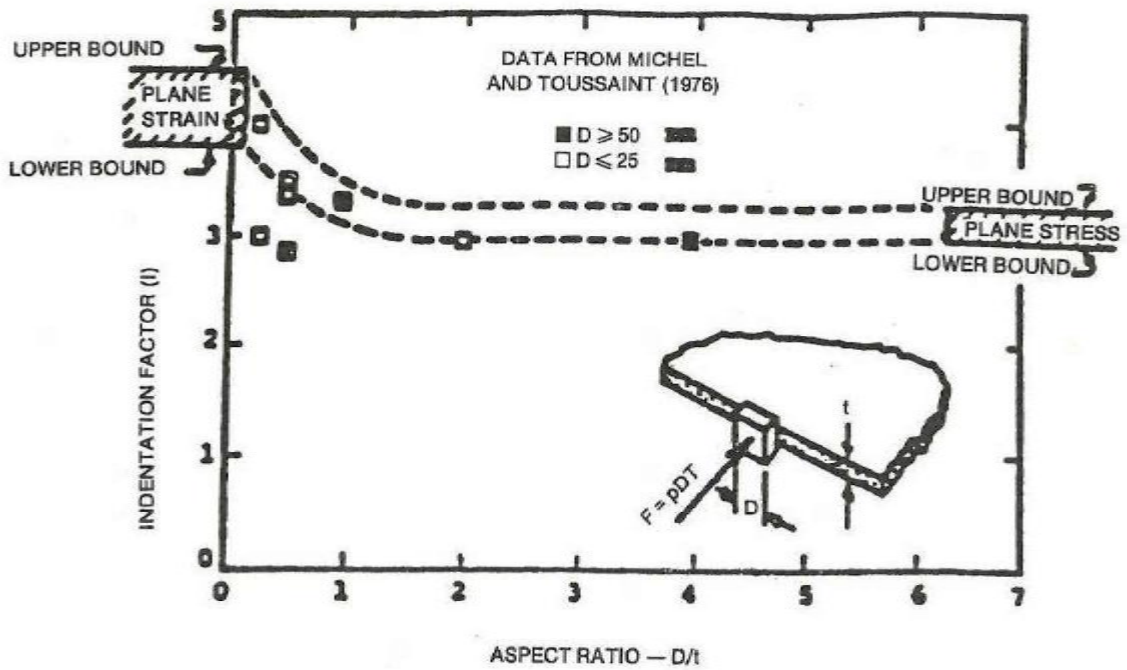
Figure 16. Comparison of computed bounds indentation factor with test data for columnar ice. [30]

Sheet or floe Bending

For slope-sided structures, sheet ice moving against s a structure may fail in bending.

A limit analysis solution for sheet ice upward bending failure against a conical structure (Figure) has been developed by Ralston. This solution includes force components for ice breaking and ice ride-up on the structure. Forces may be calculated:[30]

$$R_h = \left[A_1 \sigma_F t^2 + A_2 \rho_w g t D^2 + A_3 \rho_w g t_R (D^2 - D_T^2)\right] A_4 \tag{36}$$

$$R_v = \left[B_1 R_h + B_2 \rho_w g t_R (D^2 - D_T^2)\right] \tag{37}$$

In which:

$\left[A_1 \sigma_F t^2 + A_2 \rho_w g t D^2\right] A_4$ is the horizontal component of the force required to cause the ice to fail in bending;

60

$\left[A_3\rho_w g t_R(D^2 - D_T^2)\right]A_4$ is the force due to ice friction on the surface of the structure;

B_1R_h is the vertical component of the force required to cause the ice to fail in bending;

$\left[B_2\rho_w g t_R(D^2 - D_T^2)\right]$ is the weight of ice on the structure surface.

R_h horizontal force;

R_v vertical force;

ρ_w unit mass of water;

σ_F sheet ice bending strength;

t   ice sheet thickness;

t_R ice ride-up thikness;

D   waterline diameter of the cone;

D_T top diameter of cone;

g   acceleration of gravity;
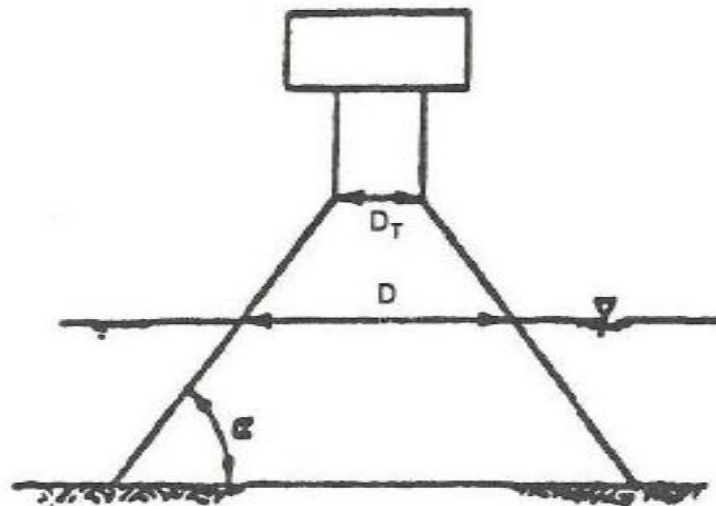
Figure 17. Cone structure geometry. [30]

The dimensions coefficients A_1, A_2, A_3, A_4, A_5, B_1, B_2 are given in Figure 17.
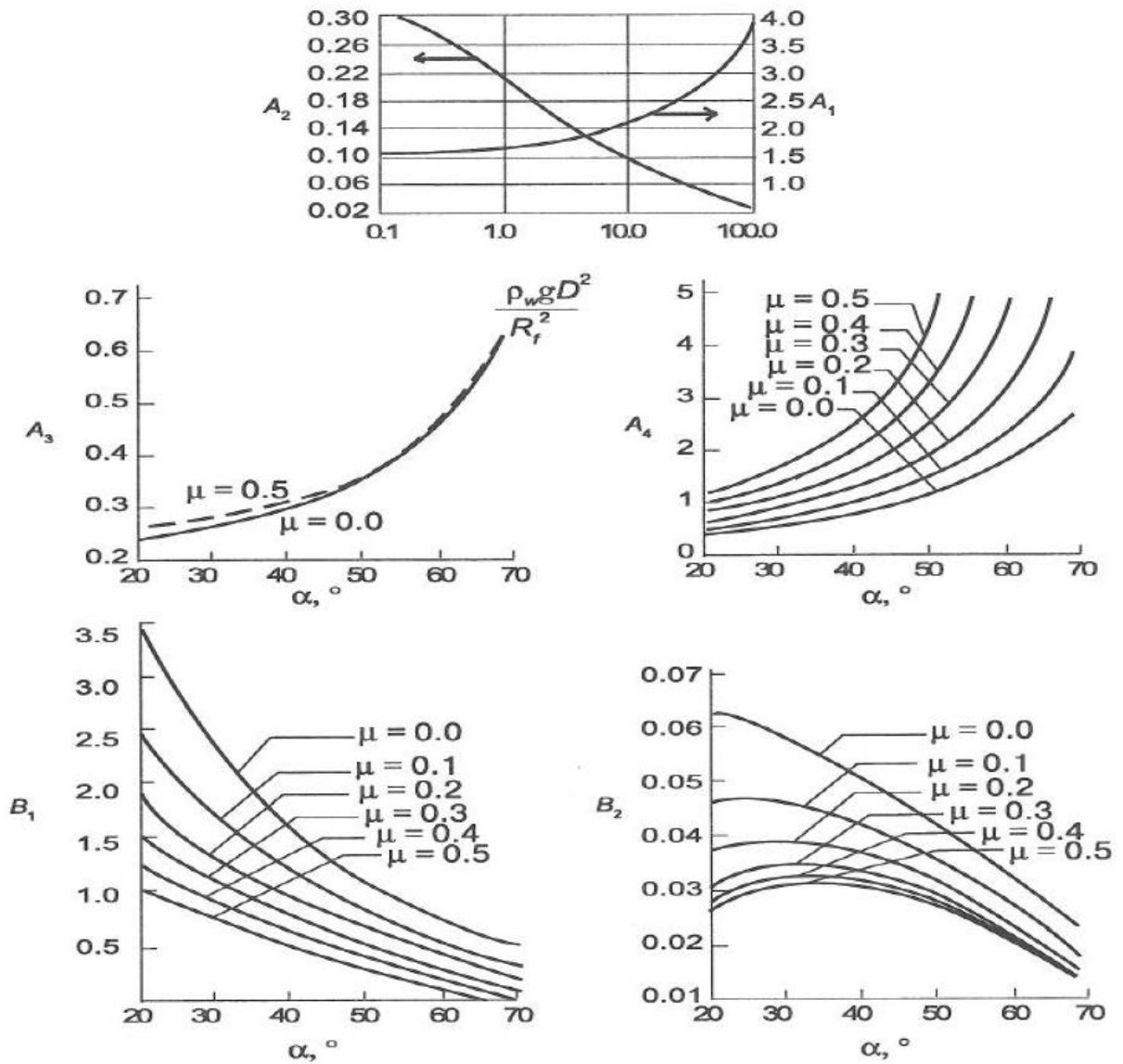
Figure 18. Ice force coefficients for plastic analysis. [30]

CHAPTER 3. ICE-RESISTANT GRAVITY BASED STRUCTURE SIMULATION IN ORCAFLEX SOFTWARE.

3.1. Brief description of the OrcaFlex Software

OrcaFlex (version 9.6a) is a marine dynamics program developed for static and dynamic analysis of a wide range of offshore systems, including all types of marine risers (rigid and flexible), global analysis, moorings, installation and towed systems. [31]

This software is fully 3 dimensional and can handle multi-line systems, floating lines, which makes extensive use of graphics to assist understanding. The program can be operated in batch mode for routine analysis work and there are also special facilities for post-processing results including fully integrated fatigue analysis capabilities. [31]

To analyze a marine system using OrcaFlex, firstly a mathematical model should be built of the real-world system, using the different modelling facilities. The model consists of the marine environment to which the system is subjected, plus a variable number of objects chosen by the user, placed in the environment and connected together as required. The objects represent the structures being analysed and the environment determines the current, wave excitation to which the objects are subjected.

The following types of objects are available in OrcaFlex:

1. **Vessels** - type of object that are used to model ships, platforms, barges.
2. **Lines** - catenary elements used to represent pipes, flexible hoses, cables, mooring lines.
3. **Links** - mass-less connections linking two other objects in the model.
4. **Winches** - mass-less connections linking two (or more) objects in the model. The connection is by a winch wire, which is fed from and controlled by a winch drive mounted on the first object.

5. **Shapes** - geometric shapes (cuboids, planes and cylinders). There are two types available – Solids or Trapped Water.

Trapped Water Shapes can be used to model parts of the sea, such as moonpools, that are shielded from the waves. Solids can be used to act as physical barriers to restrict the movement of the other objects in the system; they are made of an elastic material and so apply a reaction force to any object that penetrates them. [31]

Presented software has no ability exactly represent every aspect of a real-world system. The first model of a system might be quite simple, only including the most important aspects, so that early results and understanding can be gained quickly. Later, the model can be extended to include more features of the system, thereby giving more accurate predictions of its behavior, though at the cost of increased analysis time.[31]

When the model has been built, OrcaFlex offers a diversity of analyses:

1. <u>Modal analysis</u>, in which software calculates and reports the undamped natural modes of the model, or of an individual line in the model.
2. <u>Static analysis</u>, in which software calculates the static equilibrium position of the model; current and wind loads are included, but not wave loads.
3. <u>Dynamic analysis</u>, in which software carries out a time simulation of the response of the system to waves, current and a range of user-defined inputs. A choice of implicit and explicit integration scheme is offered.

3.2. Platform Concept selection

The platform concept selection depends on many conditions. It can be divided into two main groups: "Design and architecture type" and "Field development concept". [35]

"Design and architecture type" includes following aspects: "Operation Conditions", taking into consideration ice, waves, wind, current water depth, soils

and "Technical parameters", which is based on drilling depth, completion type, sea endurance and service life.

Another part of the platform concept selection is a "Field development Concept". Basically, it depends on regional infrastructure, production basis, manpower, capital investments, field development schedule, processing infrastructure. (see Figure 18)
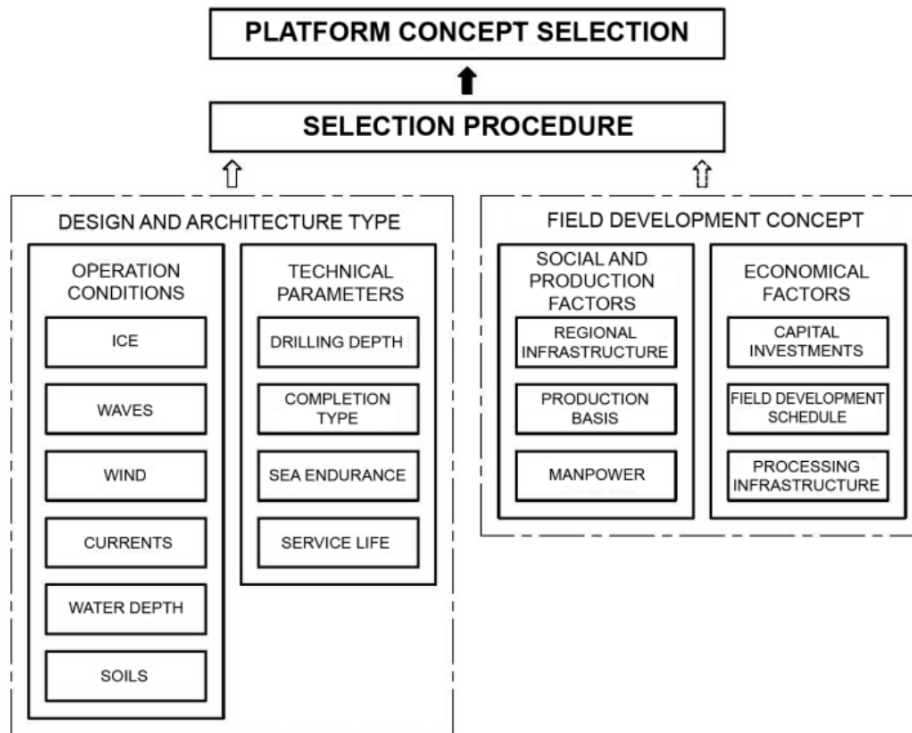
Figure 19. Factors affecting concept selection. [31]

Based on the operation conditions (water depth, ice occurrence) and technical parameters I have chosen a gravity based platform to be analyzed and simulated in Orcaflex Software. Water depth in the area (Block 708, noted with red circle, see Figure 17) allows us to use an ice-resistant gravity based structure, as a main facility for drilling, production and production storage.

There are 4 analogues (Sakhalin 1, Sakhalin 2 (Lun A), Prirazlomnoye and Hibernia) that are already in the operation, which are more or less in the similar environmental conditions. In the Figure 18 are shown the Arctic development concepts with regard to water depth.

I am interested in the Bottom founded structures, in particular, in the concrete gravity based structures, because this type of platform allows and ensures drilling and production operations during a year on the permanent base. A collision with iceberg could be considered as a risk for the platform.

Figure 20. Block 708 is considered area for drilling and production operation.

3.3. Scenario formulation

In order to calculate ice loads impact to the considered gravity based structure following assumptions were accepted:

A gravity-based, rigid arctic offshore structure is located in the shallow Barents Sea in 50m water depth. The structure is in moving ice away from lanfast ice and subjected to winter ice interactions from first-year level ice. There is no grounded ice rubble around the structure. The structure is not frozen in ice, but covered with a low friction coating. Two structural shapes (1, 2) and one ice load scenario (a) were considered:

1. Vertical-sided Square shaped structure, 100 m on each side.
2. Slope-sided structure which is also 100 m side square at the waterline. Each side has a flat 60 slope.

66

a) The 0,5 m thick first-year level ice has a drift velocity 0,5 m/s. The top surface temperature of the ice is -18 ^{O}C, the lower surface is at -2^{O}C. Salinity 3ppt.

3.4. Input for Ice Load Calculations

Different methods (standards) for determining ice loads have now been presented in the Chapter 2. Some input parameters have been defined based on literature and design basis for the platform. Table 10 gives a summary of all the user-defined parameters.

Table 10. Main input data for ice load calculations.

Parameter	Symbol	Value	Unit
Environmental parameters			
Acceleration of gravity	g	9,81	[m/s^2]
Density of sea water	ρ_w	1025	[kg/m^3]
Density of air	ρ_a	1,225	[kg/m^3]
Maximum wind speed	V_w	39	[m/s]
Water depth at location of platform	d	50	[m]
Platform dimensions			
Waterline diameter	D	100	[m]
Top diameter of the cone	D_t	80	[m]
Slope angle	α	60	[deg]
Level ice parameters			
Friction coefficient	μ	0,3	-
Density of ice	ρ_i	720	[kg/m^3]
Flexural strength of ice	σ	500	[kPa]
Elastic modulus of ice	E	5	[GPa]
Poisson ratio	ν	0,3	-
Level ice thickness	h	0,5	[m]
General			
Ice drift speed	V	0,5	[m/s]

3.5. Global ice loads estimations

Table 11 (below) shows the summary results obtained from ice load calculations on a square structure 100m wide. Detailed step by step algorithms are given in Appendix B, C, D, E.

Table 11. Summary table of ice load calculations.

№	Code	Horizontal force [MN]	Vertical Force [MN]
1	API 2N RP	10,10	8,50
2	SNIP 2.01.07-85	11,68	6,75
3	VSN 41.88	12,08	3,30
4	ISO 19906	16,87	9,34

Discussion

The following standards for ice load action estimations are studied in details:

- American Code API RP-2N (1995);
- European Code ISO 19906 (2010);
- Russian Codes SNIP 2.01.07-85, SNIP 2.06.01-86 and VSN 41.88.

All these standards and rules give more or less step-by-step guidelines to evaluate possible ice load that can be imposed on the platform. But all of them are based on different assumptions, design criteria and therefore can't give precise data about the ice effect.

The Russian code SNiP considers cylindrical and polygonal shaped structures and specifies the influence of notch shape on the action. The SNiP divides structures on two groups: a single vertical support and a section of a wide structure. The difference between the actions on the structure is large. The codes CAN/CSA, API and SNiP consider both limit force and limit momentum scenarios, whereas VSN considers only the first.

API recommends different methods for action calculation for a limit stress scenario: modified Korzhavin method, the Reference Stress and Measured Ice Pressure. Both SNiP and VSN codes are based on Korzhavin's method.

For the considered scenario ice loads due to level ice, the API 2N RP, SNIP 2.01.07-85, VSN 41.88 give loads of the same magnitude. Much bigger results are seen for ISO 19906. The reason for this may be connected to the underlying theory applied (plastic method for cones, see Chapter 2.1.7).

SNiP is mainly based on measurements on bridge piers in Russia, but often used in comparison to offshore codes, it provides deterministic design equations with unknown safety level. API 2N RP is widely based on qualitative treatment of measurements from Canadian Arctic in the 80's, while ISO 19906 is a first international standard developed, was the most comprehensive process to date and represent consensus in industry, it contains a normative part providing requirements and recommendations. Canadian Standards is based on the same measurements as used in API RP-2N, however treated with statistical and reliability theory. It provides both guidance for deterministic and probabilistic design methods.

The main difference between Russian and Western standards is a range of the considered ice strength. In Russian standards ice strength is recommended to be considered in the range of 0,3-1,5 MPa, while in ISO 19906 the strength parameter can be assumed as 2,8 MPa. Canadian Standard suggests computing ice strength using additional parameters as brine volume and nominal contact area. API 2N RP suggests to use ice strength equal to 2,5 MPa. Such differences directly impact to horizontal, vertical forces and global loads to the structures. (See Appendix B-E)

There is no right answer which standard is better to use. SNIP 2.01.07-85 and VSN 41.88 are used in Russia, while API 2N RP is used in the USA, Canadian one is used more likely in Canadian arctic offshore and ISO 19906 is used in Europe.
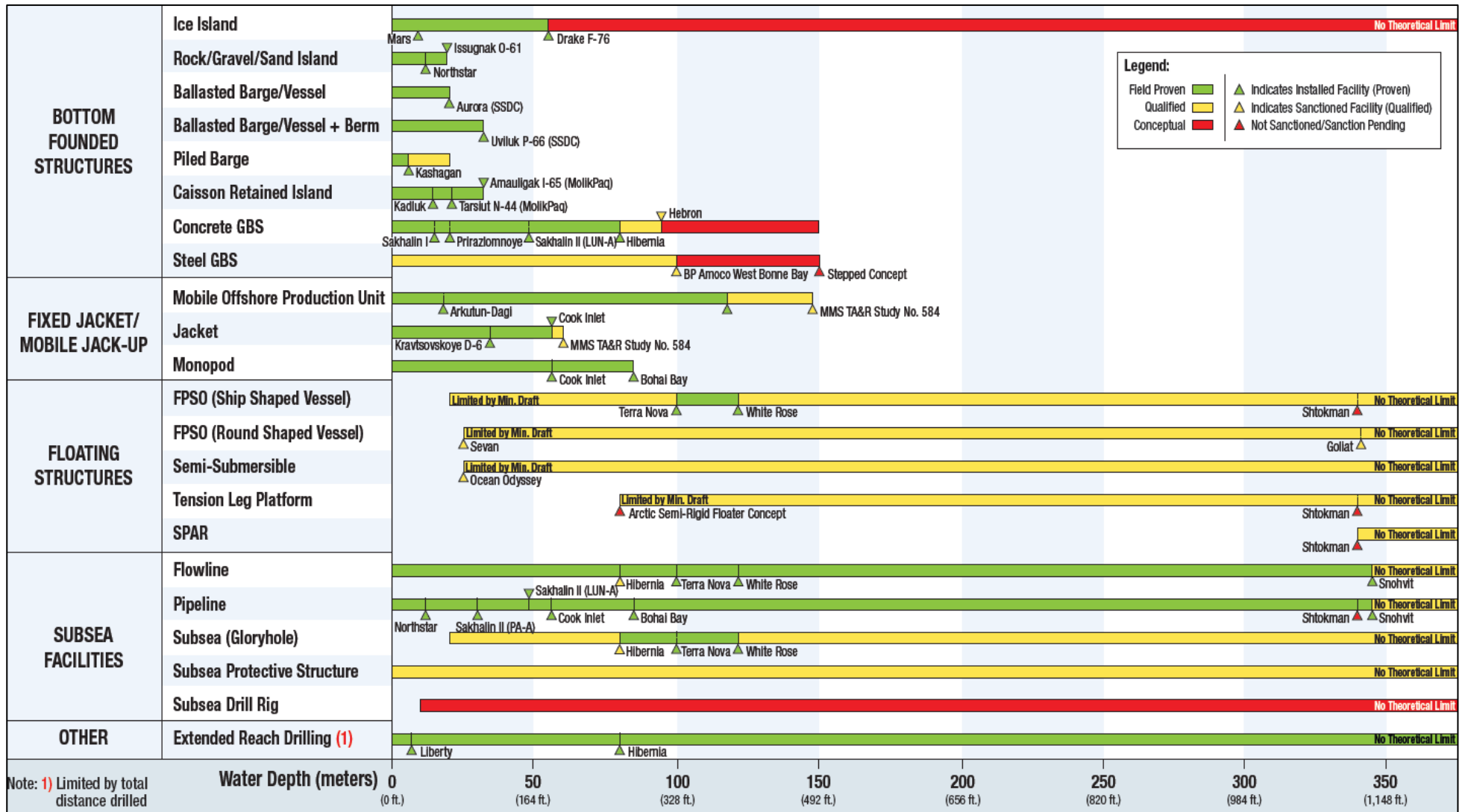
Figure 21. Arctic development concepts water depth ratings (taken from http://www.offshore-mag.com/)

3.6. Platform simulation results

3.4.1. Vertical-sided platform design

This paragraph describes simulation philosophy of the gravity based structure that was selected as a best option for exploration drilling in the Block 708 in Norwegian sector of the Barents Sea. Below are given the results of the simulation (see Figures 21-33). Figures 21-27 show images of the vertical-sided ice-resistant gravity based platform design during ice drift.

Seabed Shape Data

Three types of seabed shape have been available during simulation:

- A Flat seabed is a simple plane, which can be horizontal or sloping;
- A profiled seabed is one where the shape is specified by a 2D profile in a particular direction. Normal to that profile direction the seabed is horizontal.
- A 3D seabed allows you to specify a fully general 3D surface for the seabed, by specifying the depth at a series of X, Y positions with a choice of linear or cubic polynominal interpolation in between. [31]

In our case a Flat seabed shape has been selected, because of lack of information related to the seabed profile in the Finnmark area.

3D views.

As a result of the simulation I have gotten 3D views that are windows showing a spatial representation of the model. Two distinct types of 3D have been created:

1. Wire frame (Figures 21, 22 23, 28, 29, 30) shows an isometric projection of the model.
2. Shaded pictures (Figures 24, 25, 26, 27, 31, 32, 33) are the models as solid objects with lighting, shading, perspective and hidden line removal.

All obtained 3 dimensional views of the platform with different wall shapes give better understanding of the presented ice drift scenario.
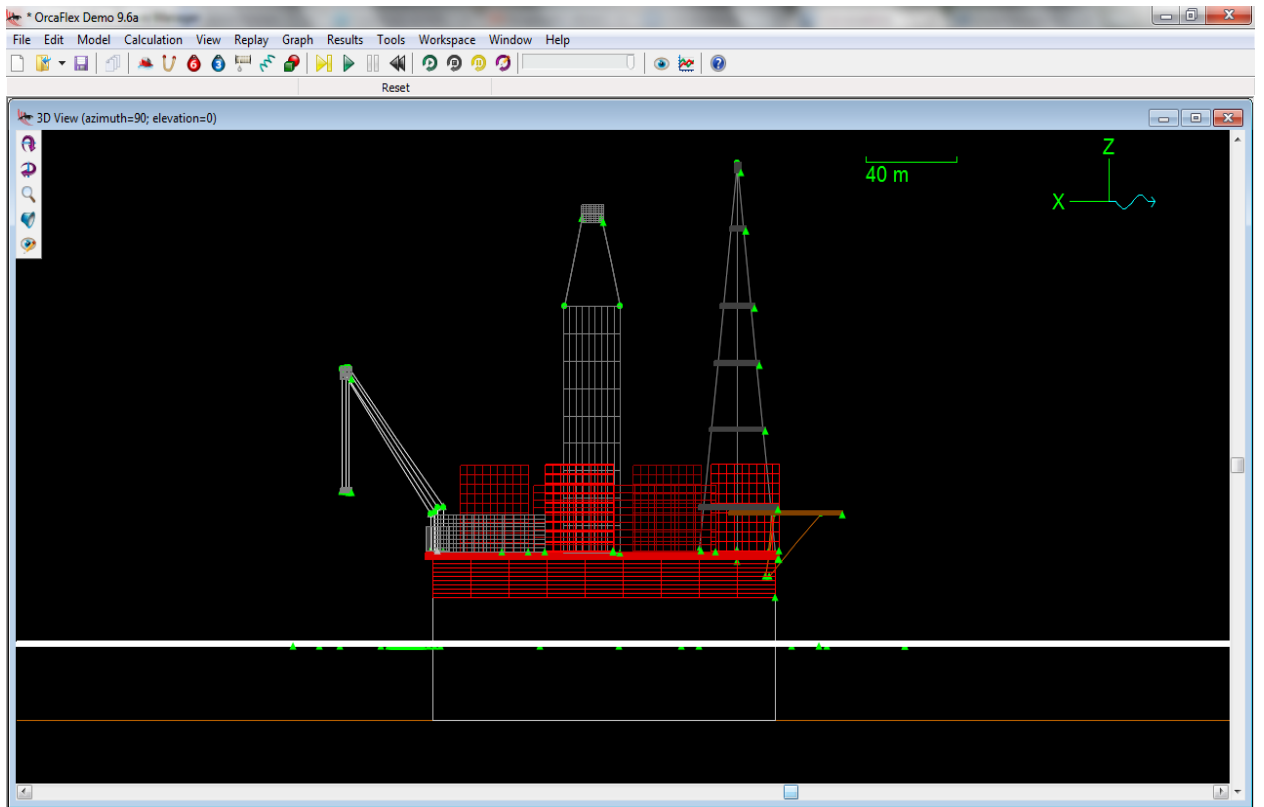
Figure 22. Front view to ice-resistant gravity based platform.

Figure 23. Side view to ice-resistant gravity based platform.
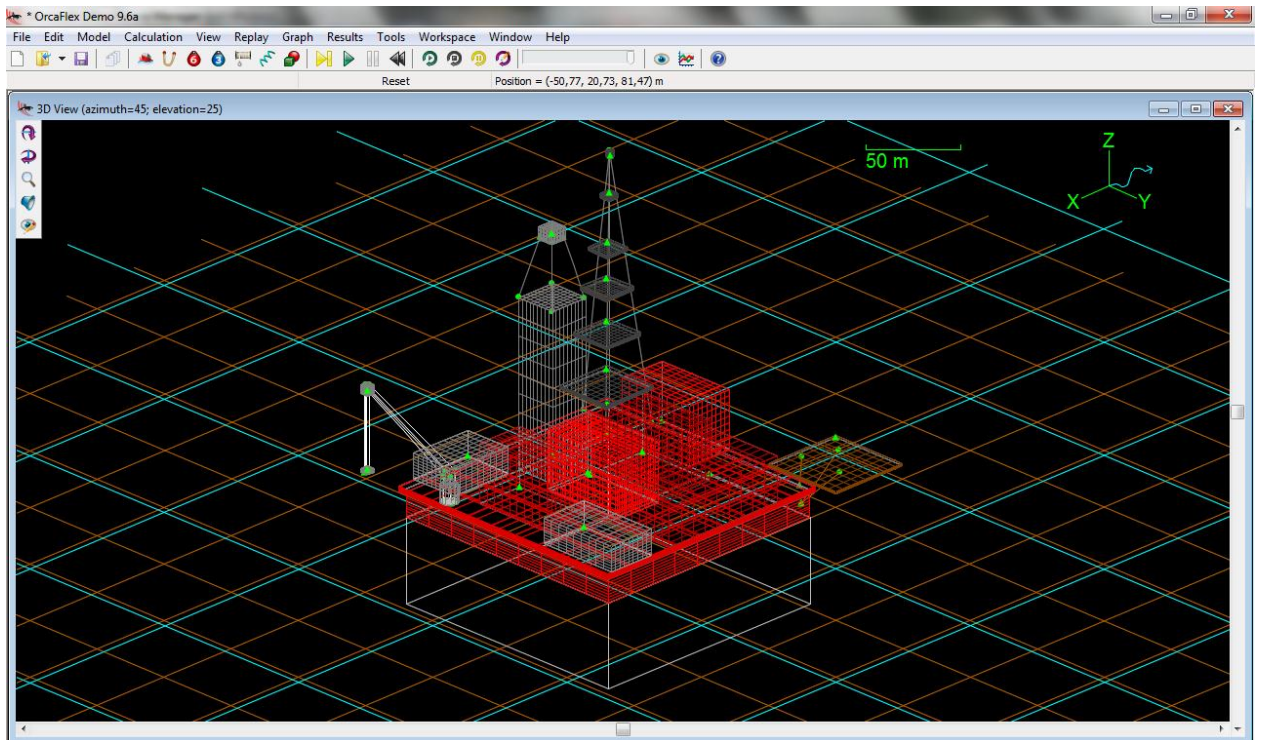
Figure 24. 3D view to ice-resistant gravity based platform.
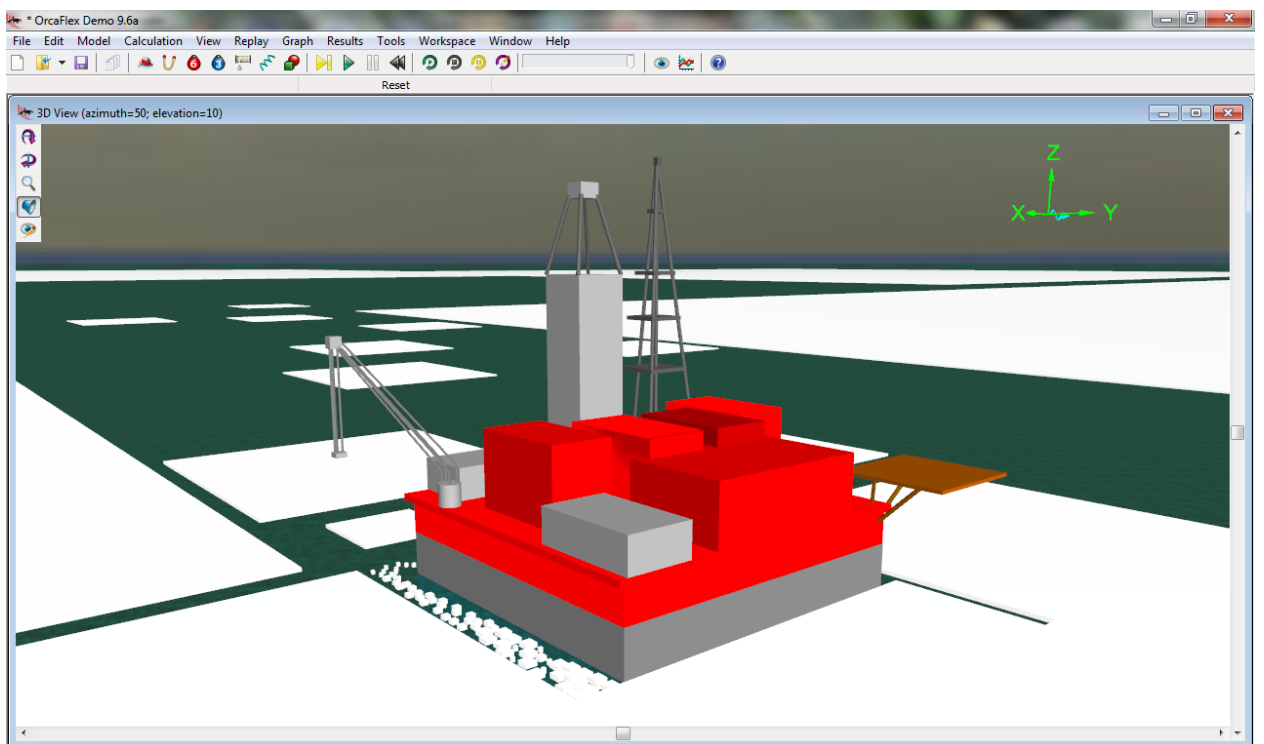
Figure 25. 3D view ice-resistant gravity based platform, ice drift direction from diagonal at lower right to left.
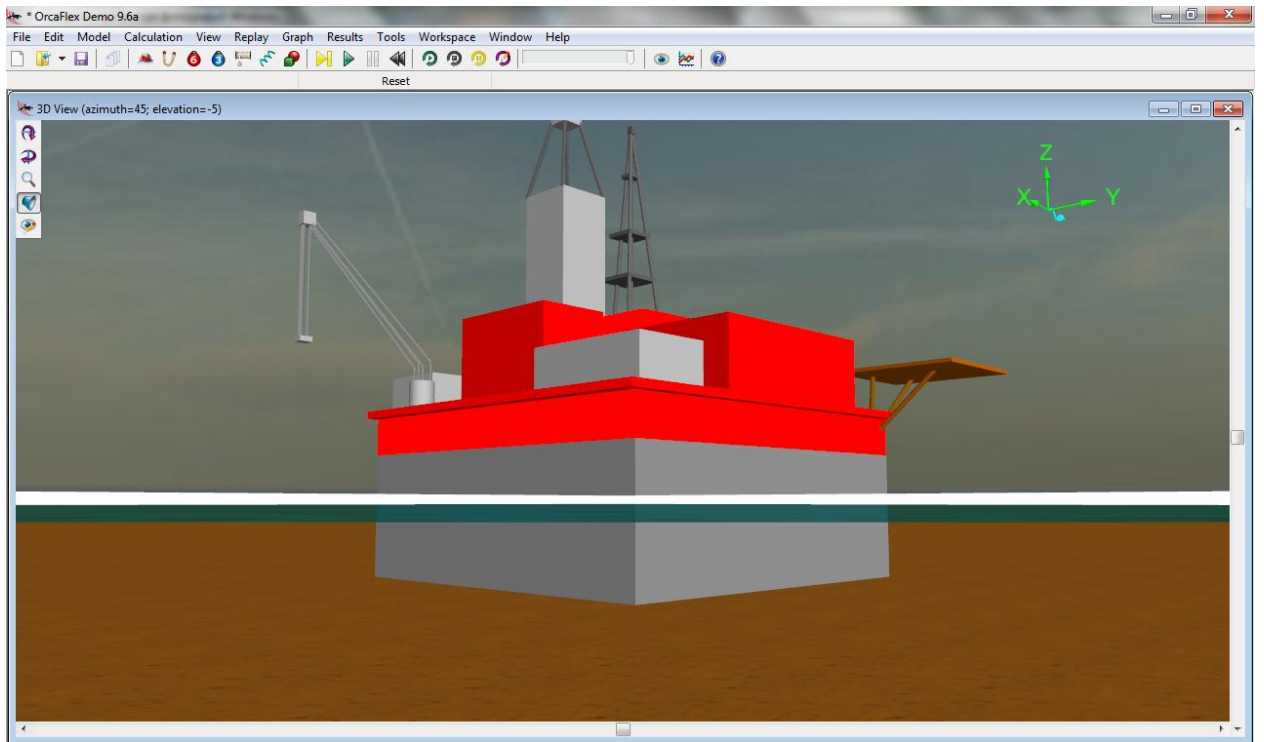
Figure 26. View from the sea surface to ice-resistant gravity based platform.
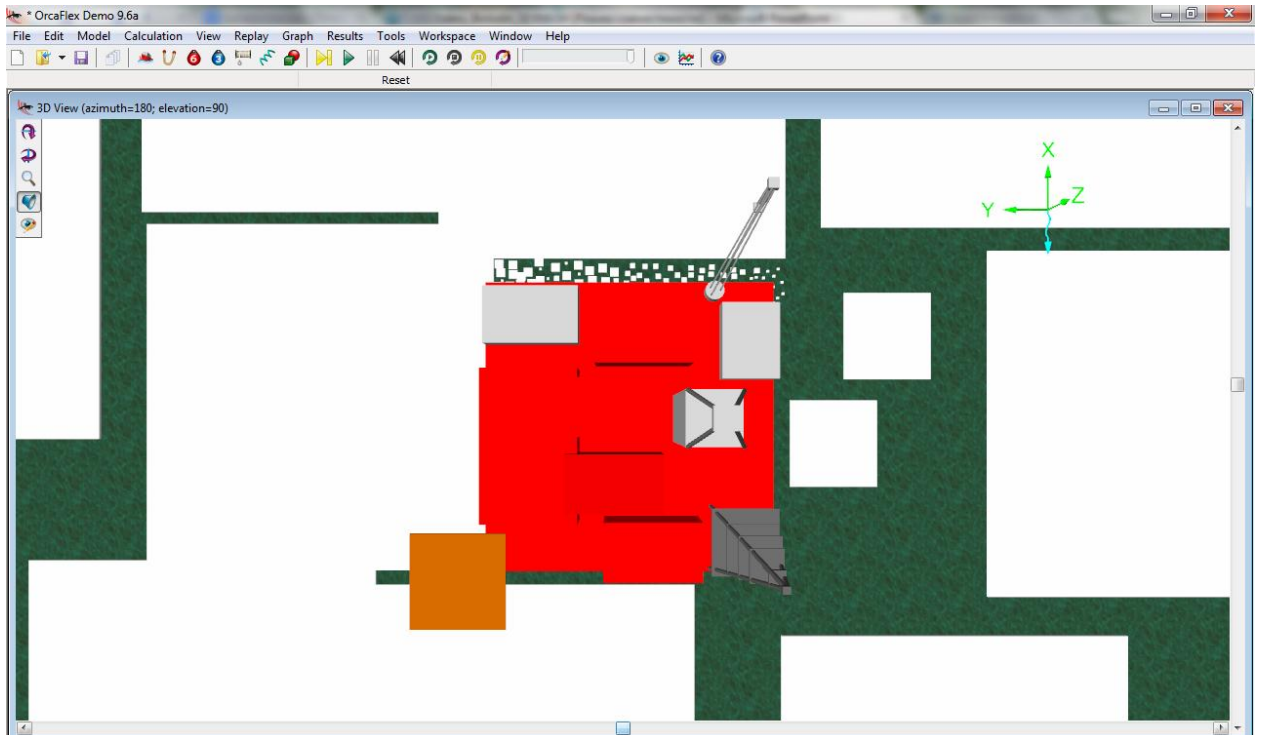
Figure 27. Top view of ice-resistant gravity based platform, ice drift from left to right.
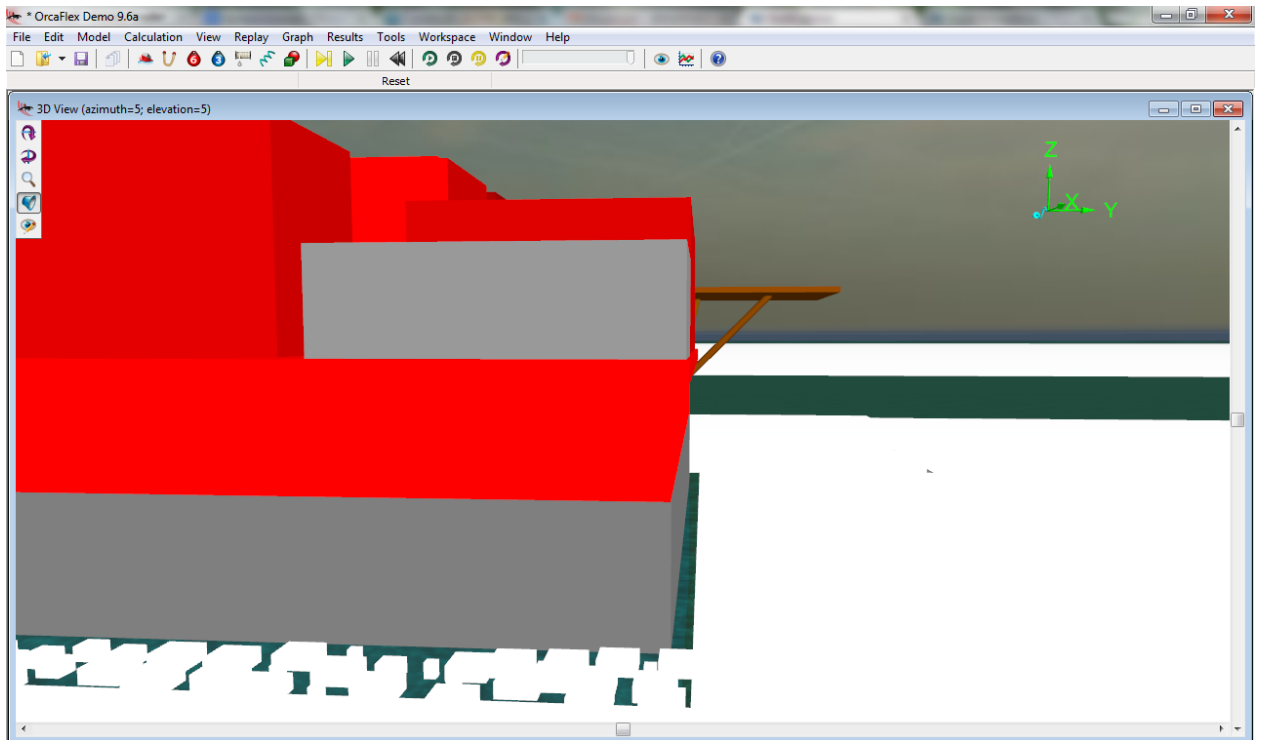
Figure 28. 3D View of vertical walls of the ice-resistant gravity based platform.

3.4.2. Sloped-sided platform design

Figures 28-33 show images of ice drift on the sloped-sided ice-resistant gravity based platform design.
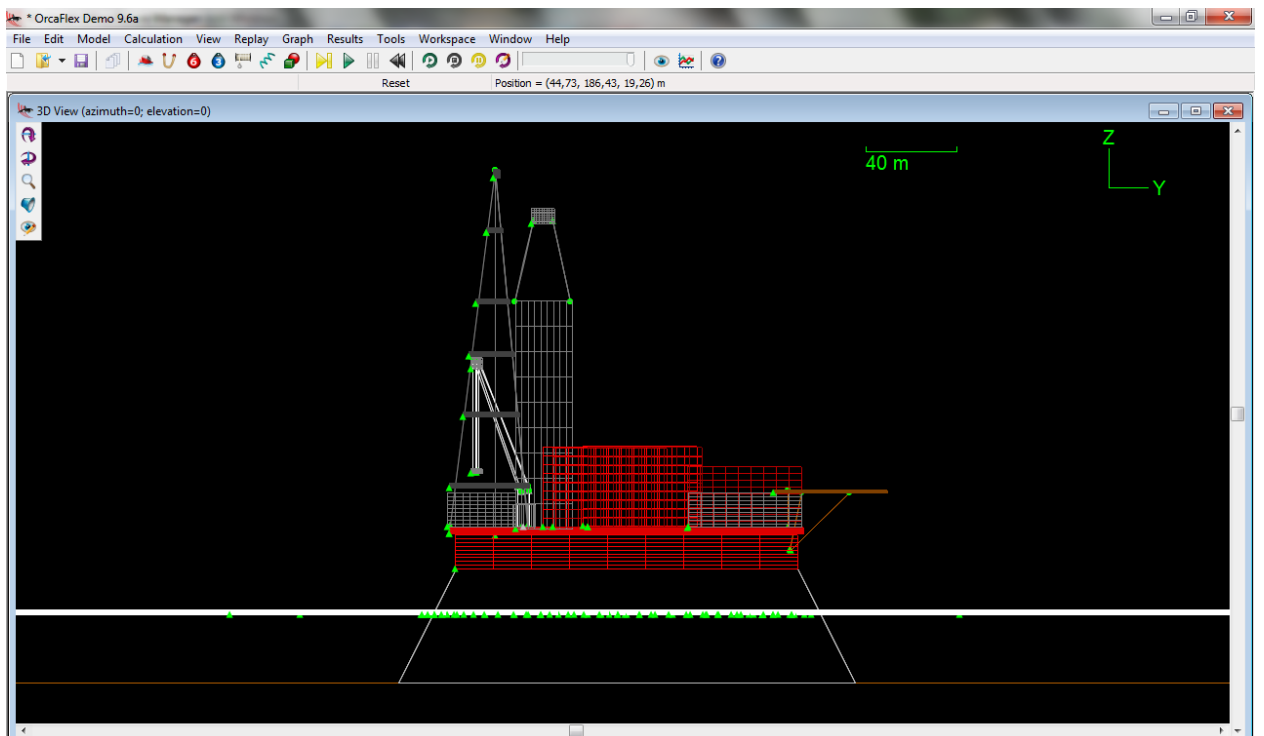
Figure 29. Front view to ice-resistant gravity based platform.
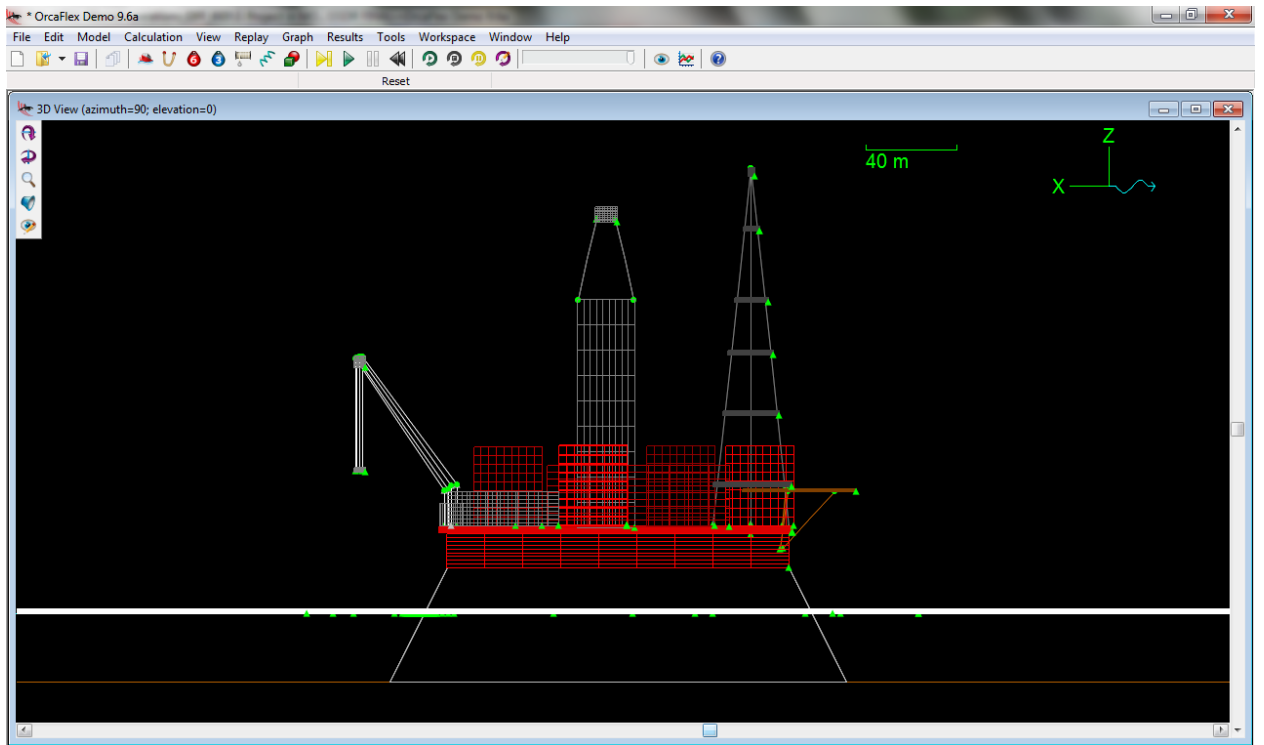
Figure 30. Side view to ice-resistant gravity based platform.

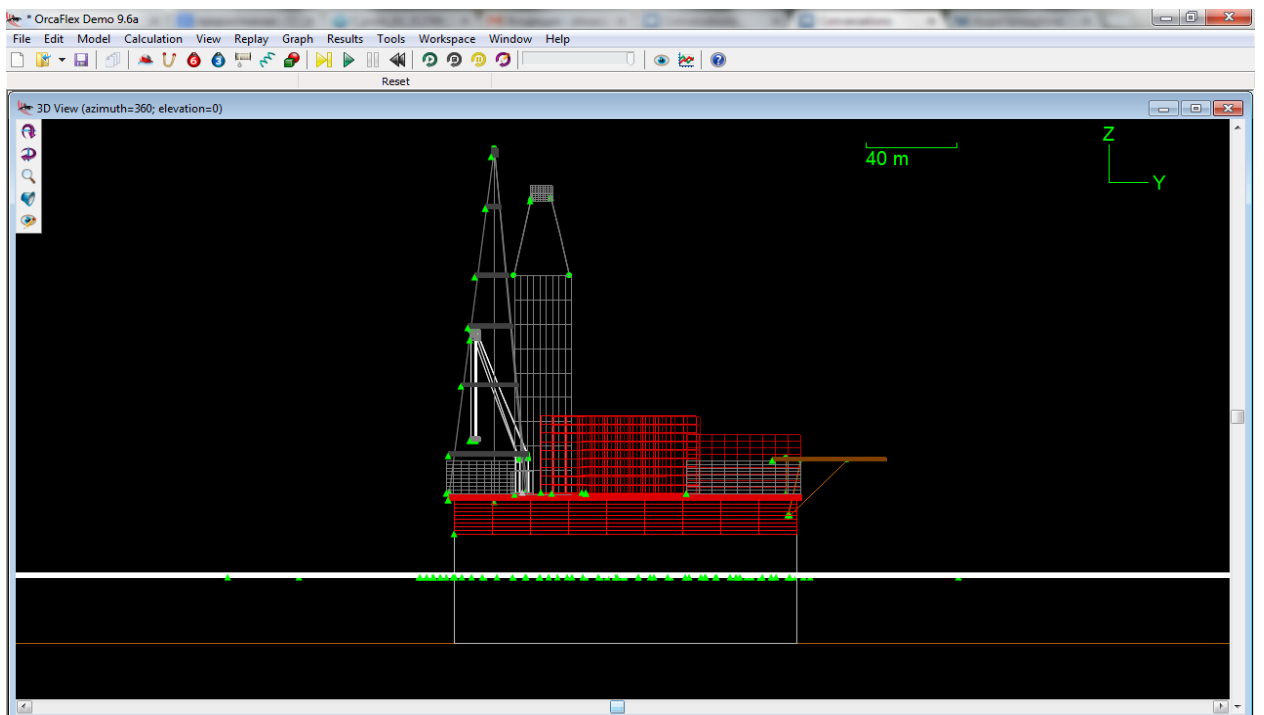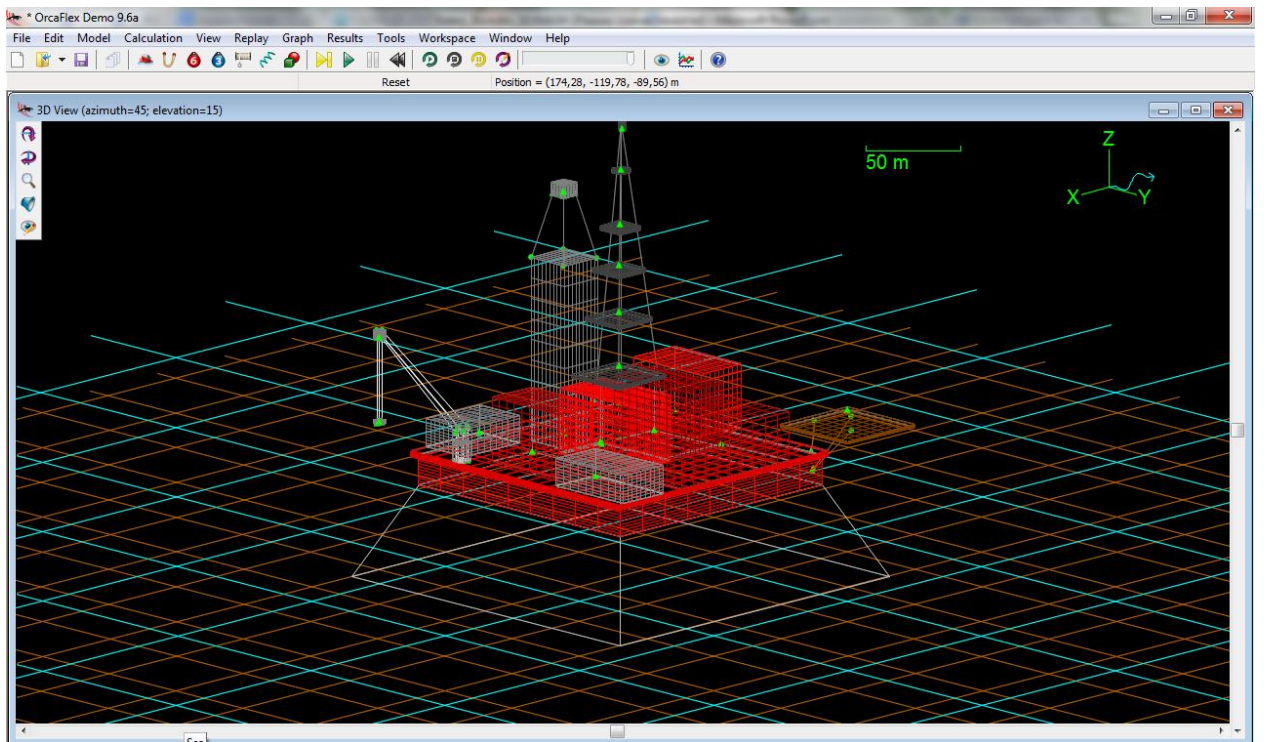**Figure 31. 3D view to ice-resistant gravity based platform.**
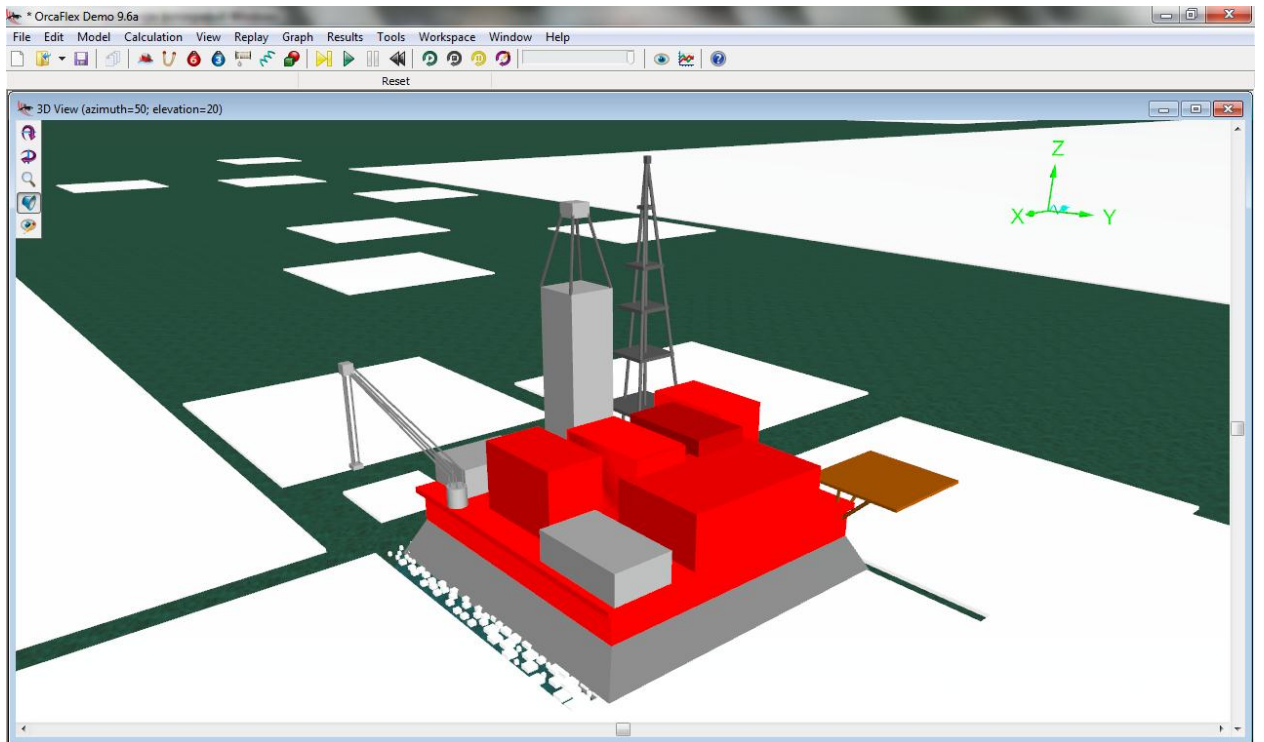
Figure 32. 3D view to ice-resistant gravity based platform, ice drift direction from diagonal at lower right to left.
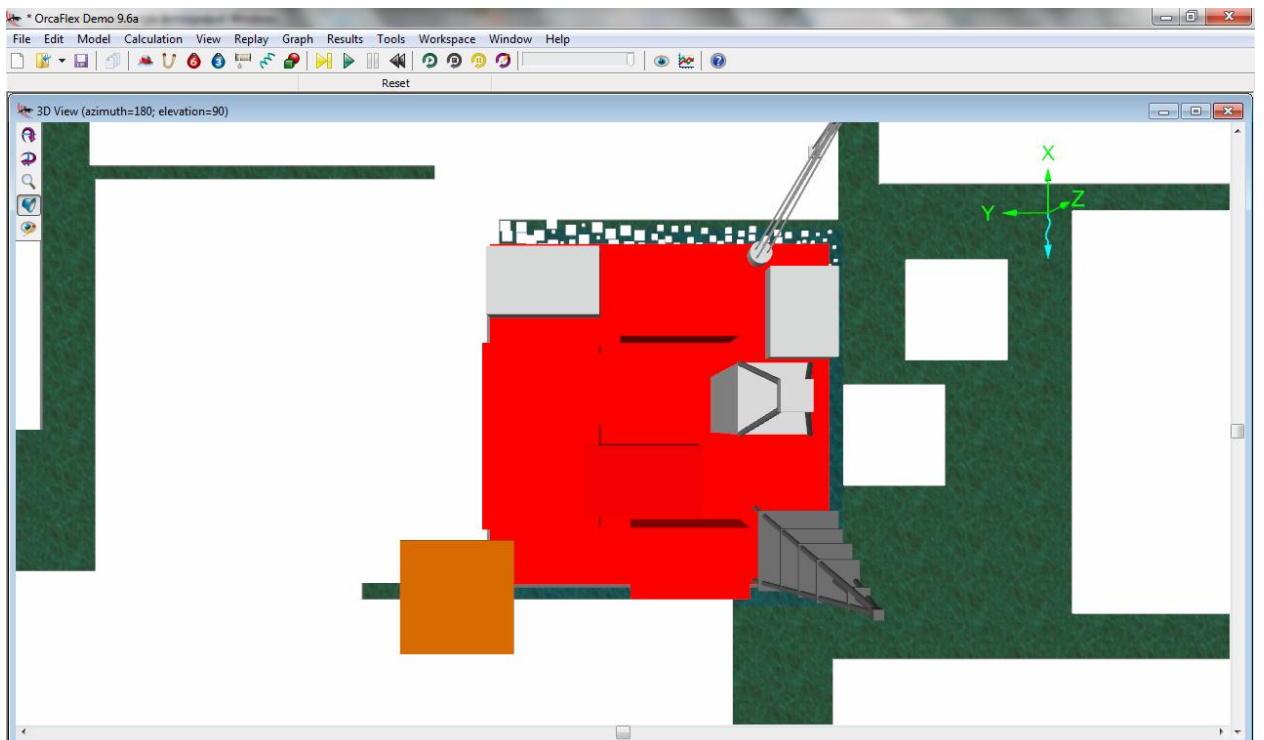
Figure 33. Top view to ice-resistant gravity based platform, ice drift from left to right.
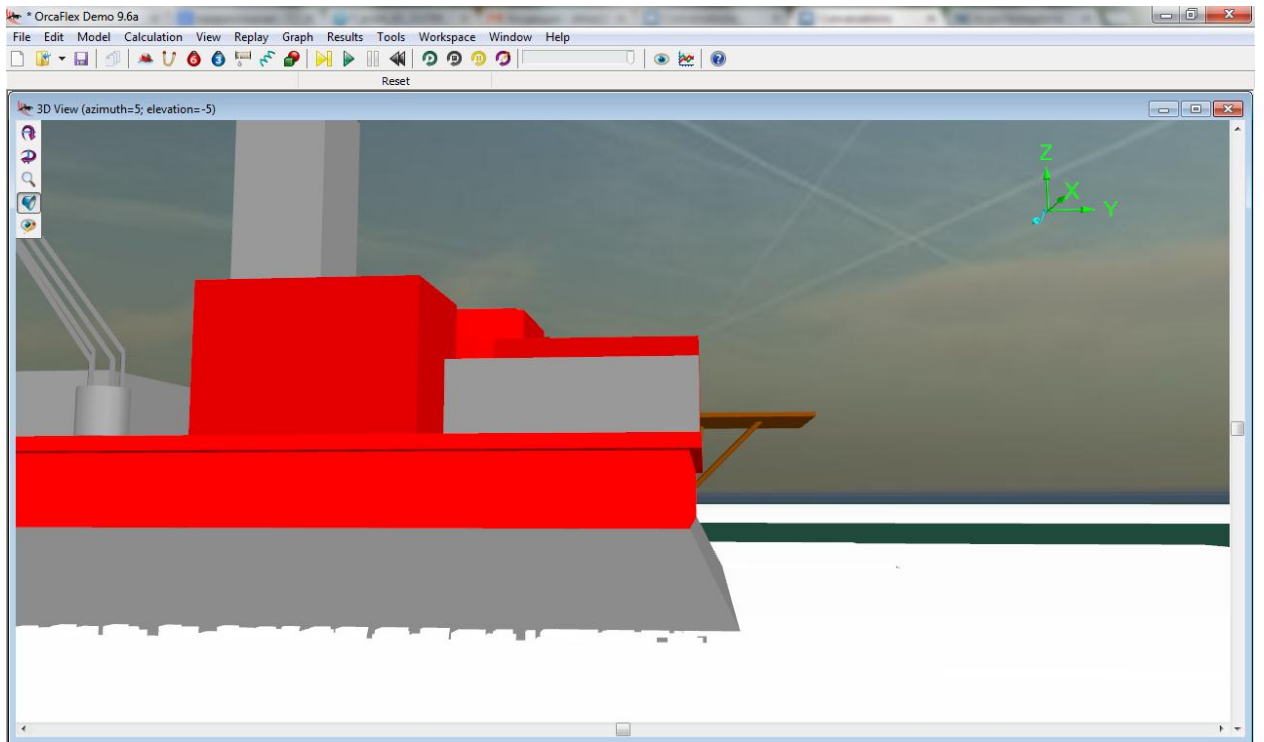
Figure 34. 3D View to sloped walls of the ice-resistant gravity based platform.

CHAPTER 4. RISK ANALYSIS.

4.1. Introduction

A qualitative risk analysis prioritizes the identified project risks using a pre-defined rating scale. Risks will be scored based on their probability or likelihood of occurring and the impact on project objectives should they occur. Probability/likelihood is commonly ranked on a zero to one scale.

The impact scale is organizationally defined (for example using a one to five scale, with five being the highest impact on project objectives - such as budget, schedule, or quality).

A qualitative risk analysis will also include the appropriate categorization of the risks, either source-based or effect-based. [32]

Qualitative risk analysis

Qualitative risk analysis includes following aspects:

1. Accept criteria;
2. Hazid (Hazard Identification);
3. Risk Analysis;
4. Risk Reduction;

   - Non Acceptable;
   - As low as reasonable practical (ALARP);
   - Acceptable.[33]

Tables 12 and 13 below show Lukoil's Risk matrix and description that are considered during risk analysis within development of oil and gas fields. There is a probability rating which is divided into 5 categories:

   - Probable;
   - Remote;
   - Extremely remote;
   - Improbable;

- Extremely improbable.

All these categories are marked from 1 to 5. As well, Lukoil's Risk matrix considers "Severity Rating", which is divided into catastrophic, major, serious, minor and negligible risky situations. They are marked as A, B, C, D, E. Low, Medium, High and Extreme indicators correspond to the Risk Level.

Acceptable risk is indicated with white color in table 12 below. It is a level of human and/or material injury or loss from an industrial process that is considered to be tolerable by a society or authorities in view of the social, political, and economic cost-benefit analysis. [36]

In my case I assumed that following HAZIDS: flow rate increase, elliptical hole, unexpectedly high rate of penetration, torque/ drag increase are considered as Acceptable Risks. (see Chapter 4.2)

Table 12. Lukoil's Risk Matrix.

		1	2	3	4	5
Low	**E**	M	M	L	L	L
	D	M	M	M	L	L
Severity	**C**	E	H	M	M	L
	B	E	H	H	M	M
High	**A**	E	E	H	H	M

High　　　　　　　　**Probability**　　　　　　　　**Low**

Table 13. Lukoil's Risk Matrix descriptions.

	Probability rating		Severity rating	Risk Level
1	Probable	A	Catastrophic	Low
2	Remote	B	Major	Medium
3	Extremely remote	C	Serious	High
4	Improbable	D	Minor	Extreme
5	Extremely improbable	E	Negligible	

4.2. Hazid to identify the risk during drilling operation

Hazard identification (HAZID) is "the process of identifying hazards, which forms the essential first step of a risk assessment". [34].

Let us make a HAZID list which possibly can occur during drilling operation:

1. Fluid loss;
2. High bit wear;
3. Unexpectedly high rate of penetration;
4. Torque/ drag increase;
5. Flow rate increase;
6. Cavings;
7. Shut-in drill pipe pressure;
8. Unexpectedly low rate of penetration;
9. Elliptical hole;
10. Bottom hole assembly drift.

All described Hazids have been filled in into the Risk matrix (Table 14).

Table 14. HAZID to identify the risk during drilling.

Severity		1	2	3	4	5
Low	E					
	D			4,9	3,5	
Severity	C		6,7			
	B			1,8		
High	A	10	2			

	High	Probability	Low

4.3. Bow tie analysis

To carry out a bow tie analysis, let us identify barriers and ensure that a sufficient number of barriers are in place for issues where the risk is high. Under

the term "high risk" let us consider that type of risks, which are within the dark grey (risk matrix above) area namely "Non Acceptable Risks".

Figure 31 shows the principle of bow-tie diagram, which is based on determination of potential causes, preventive and mitigative controls and consequences of a major accident.
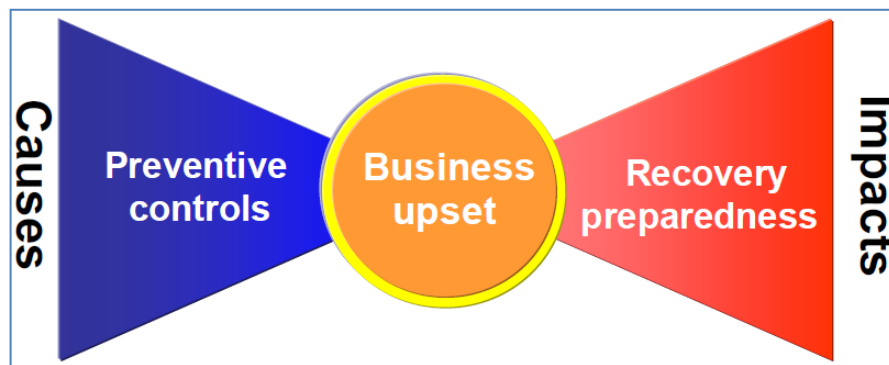
Figure 35. Principle of bow-tie diagram (taken from the "Presentation to the International Conference for Achieving Health & Safety Best Practice in Construction, Dubai, UAE, 26th-27thFebruary 2007").

Diagrams below present threats, consequences and barriers which are necessary to take into account when there is a possibility to encounter given challenges.

In the following bow-tie analysis the risks with the highest probability of occurrence and the most serious consequences are reviewed.

I have considered that following risks are "Non Acceptable Risks" in our case:

1. Bottom Hole Assembly (BHA) drift;
2. High bit wear;
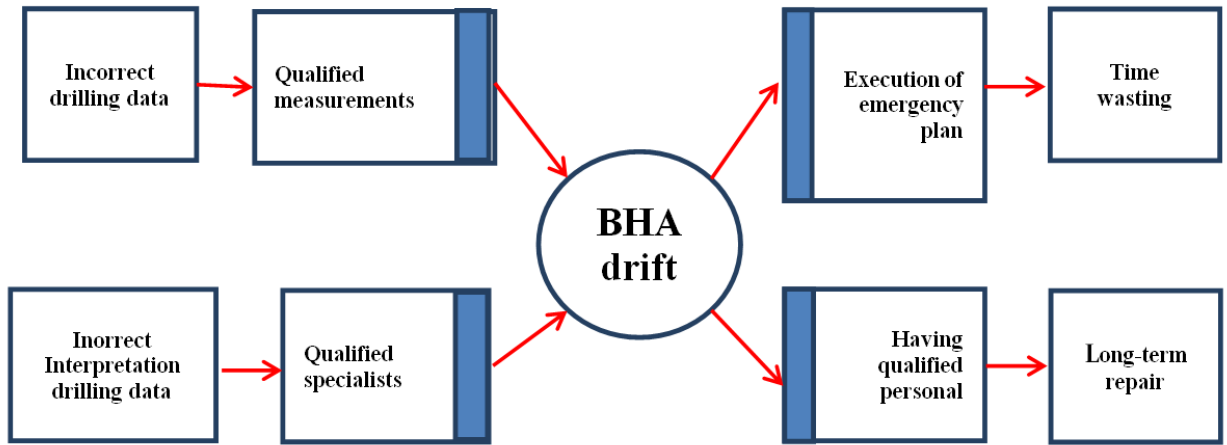
Figure 36. Bow tie diagram for "BHA drift" event.
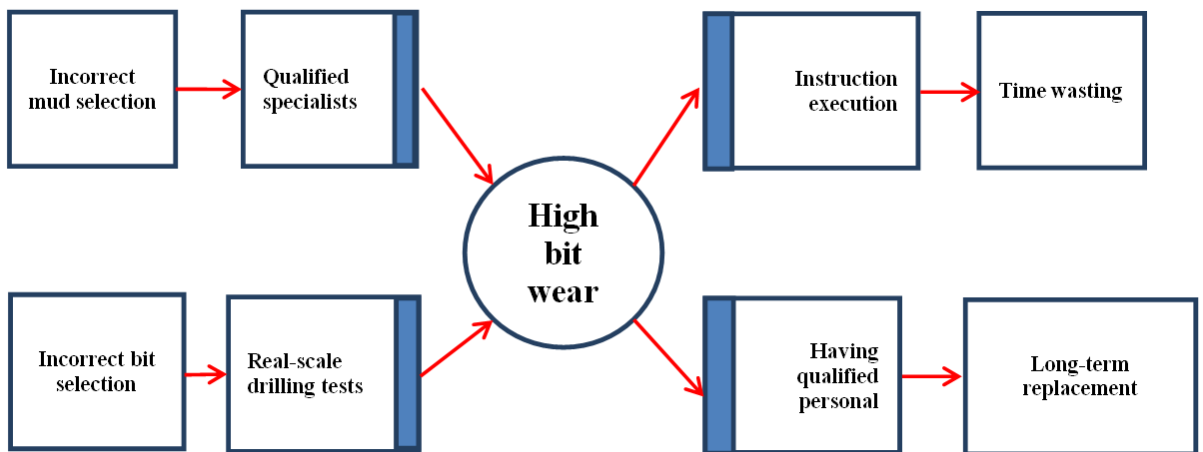
Figure 37. Bow tie diagram for "High bit wear" event.

CONCLUSIONS

The following standards for ice load action estimations are studied in details:

- American Code API RP-2N (1995);
- European Code ISO 19906 (2010);
- Canadian Code CAN/CSA (2008);
- Russian Codes SNIP 2.01.07-85, SNIP 2.06.01-86 and VSN 41.88.

All these standards and rules give more or less step-by-step guidelines to evaluate possible ice load that can be imposed on the platform. But all of them are based on different assumptions, design criteria and therefore can't give precise data about the ice effect.

Hence, below there are the main results and conclusions of the presented Master Thesis:

1. The ice resistant gravity based platform was selected as the main facility for exploration drilling in the Block 708 in the Norwegian sector of the Barents Sea due to the similarity with existing exploration and development projects offshore Sakhalin and for the Prirazlomnaya fields. Mainly similarity based on the environmental conditions. As well, this conclusion is done on the basis of ice-resistance, reliability, cost, performance, safety and environmental design of the platform.

2. Ice-resistant gravity based platform with vertical and sloped wall was simulated in OrcaFlex software to visualize ice failure and to give better understanding of the presented ice drift scenario.

3. Comparison and computation between Russian and Western codes for global ice load estimations is done.

4. Qualitative risk analysis for possible risks with the highest probability of occurrence and the most serious consequences are reviewed, based on Lukoil's risk matrix.

REFERENCES

1. International Hydrographic Organization, "Limits of Oceans and Seas" Draft 4th Edition, issued by International Hydrographic Organization,2002.

2. Matishov, G., Golubeva, N., Titova, G., Sydnes, A. and Voegele, B., "Global International Water Assessment - Barents Sea", issued by the University of Kalmar on behalf ofUnited Nations Environment Programme, 2004.

3. Gudmestad, O.T., Olufsen A., Strass P., "Challenges for the Development of Hydrocarbon Fields in the Barents Sea",The International Society of Offshore and Polar Engineers,1995.

4. Gudmestad, O.T. and Strass P., "Technological challengesfor hydrocarbon production in the Barents Sea", Proc.POAC 1993, pp. 403 - 412, Hamburg, 1993.

5. State Research Center Arctic and Antarctic Research Institute http://www.aari.nw.ru/resources/a0013_17/barents/atlas_barents_sea/_Atlas_Barenc_Sea_seasons/text/Barenc.htm

6. Gudmestad, O.T., Karunakaran, D., "Challenges Faced by the Marine Contractors Working in Western and Southern Barents Sea", OTC 23842, paper was prepared for presentation at the Arctic Technology Conference held in Houston, Texas, USA, 3-5 February 2012.

7. Noer, G. and Lien, T., "Dates and Positions of Polar lows over the Nordic Seas between 2000 and 2010", Norwegian Meteorological Institute, Report no. 16/2010

8. http://www.pennenergy.com/articles/pennenergy/2013/06/lukoil-awarded-offshore-oil-exploration-licenses-in-barents-sea.html

9. Jacobsen, S. R, "Evacuation and Rescue in the Barents Sea", Master Thesis at the University of Stavanger, 2012.

10. Norsok: N-003 Edition 2, "Actions and action effects", issued by Standards Norway, September 2007.

11. http://www.nrk.no/nordnytt/isen-kan-true-nye-oljefelter-1.7950834

12. Kvitrud, A.,"Environmental conditions in the southern Barents Sea", Paper presented in Stavanger in 1991, but put on Internet 25.9.2002.

13. Norwegian Petroleum Directorate (NPD), "Petroleum resources on the Norwegian continental shelf" 2013.

14. http://factpages.npd.no/factpages/default.aspx

15. Zolotukhin, A. and Gavrilov, V., "Russian Arctic Petroleum Resources: Challenges and Future Opportunities", OTC 22062, paper was prepared for presentation at the Arctic Technology Conference held in Houston, Texas, USA, 7–9 February 2011.

16. Norwegian Ministry of petroleum and energy, "The High North - Visions and Strategies", Meld. St. 7 (2011–2012) White paper to Parliament.

17. Norwegian Ministry of petroleum and energy, "An industry for the future – Norway´s petroleum activities"Meld. St. 28 (2011–2012) White paper to Parliament.

18. Mosesyan, M., Mukhoryamov, M., "Arctic Drilling Activities: Critical Review of the International Safety Standards, Technical Regulations and Regulatory Regimes", SPE 166973, 2013.

19. ISO 19906:2010, "Petroleum and natural gas industries, Arctic offshore structures", issued by the International Organization for Standardization, 2010

20. Gordeeva, T. S., "Identification of Criteria for Selection of Arctic Offshore Field Development Concept"», Master Thesis at the University of Stavanger, 2013.

21. "Meteorologiske og oseanografiske parametre fra kyst-, hav- og landposisjoner", prepared by DNMI, Oslo, Norway: http://www.regjeringen.no/pages/14137473/Vedlegg_12_6.pdf

22. http://en.wikipedia.org/wiki/File:Polar_low.jpg

23. ISO 19006 –"Petroleum and natural gas industries — Arctic offshore structures". Same as reference 19.

24. CAN/CSA-S471-04–"General requirements, design criteria, the environment, and loads", Canadian Standard Association, 2008.

25. SNIP-2.06.04-82 "Loads and Impact Ice on Hydraulic Structures", Gosstroy USSR, 1982.

26. VSN 41.88 - "Loads and effects of ice", Ministry of oil production, USSR, 1988.

27. Ralston, T.D., "Plastic Limit Analysis of Sheet Ice Loads on Conical Structures",IUTAM Symposium on Physics and Mechanics of Ice, ed. P. Tryde (New York: Springer-Verlag), 289–308,1980..

28. Nevel, D. E., "Ice Forces on Cones from Floes". Proceedings of the 11th International Association for Hydraulic Research Symposium on Ice 3: 1391–1404, 1992.

29. Croasdale, K.R., "Ice Forces: Current Practices". Proceedings of the 7th International Conference on Offshore Mechanics and Arctic Engineering 4: 133–151. 1998.

30. API RP 2N – "Recommended Practice for planning, designing, and constructing fixed offshore structures in Ice Environments", American Petroleum Institute, 1988.

31. OrcaFlex Manual (version 9.6a), Orcina Ltd., 2013.

32. http://www.passionatepm.com/blog/qualitative-risk-analysis-vs-quantitative-risk-analysis-pmp-concept-1

33. Gudmestad, O.T., Lectures in "Marine Operations" at Gubkin University, UiS, 2013.

34. Germanischer, L, Safety & Risk Management Services Hazard Identification Studies (HAZID), 2008.

    http://www.germanlloyd.org/pdf/Hazard_Identification_Studies.pdf

35. Livshyts B. R., Lenskiy V. F., Nesin, D Y. "Platform Design for Arctic Shallow Waters", ISSN 1098-6189, 2012.

36. http://www.businessdictionary.com/definition/acceptable-risk.html

APPENDIX A.

Table 15. Drilling activities in the Barents Sea [14]

Year	DEVELOPMENT WELL			EXPLORATION WELL	
	PRODUCTION	OBSERVATION	INJECTION	APPRAISAL	WILDCAT
1980	0	0	0	0	2
1981	0	0	0	0	3
1982	0	0	0	1	3
1983	0	0	0	1	5
1984	0	0	0	2	5
1985	0	0	0	2	5
1986	0	0	0	0	2
1987	0	0	0	0	5
1988	0	0	0	0	4
1989	0	0	0	0	4
1990	0	0	0	0	1
1991	0	0	0	0	3
1992	0	0	0	0	3
1993	0	0	0	0	2
1994	0	0	0	0	0
1995	0	0	0	0	0
1996	0	0	0	0	0
1997	0	0	0	0	0
1998	0	0	0	0	0
1999	0	0	0	0	0
2000	0	0	0	0	4
2001	0	0	0	2	2
2002	0	0	0	0	0
2003	0	0	0	0	0
2004	0	0	1	0	0
2005	8	0	0	0	3
2006	1	0	0	2	4
2007	0	0	0	1	2
2008	0	0	0	3	5
2009	0	0	0	0	0
2010	0	0	0	0	1
2011	0	0	0	0	7
2012	0	0	0	2	3
2013	0	1	3	1	9
2014	0	0	0	0	1
Total - 119	9	1	4	17	88

APPENDIX B.

In the tables below (15-20) are given the input data and results of determination of ice loads by using API RP 2N. (see the Chapter 2)

1.1. Sheet or Floe crushing

Table 16. Description of initial parameters for calculation the horizontal ice force.

Parameter	Unit	Description
t	m	ice thickness
D	m	width of the structure
I	-	indentation factor
f_c	-	contact factor
C_x	MPa	unconfined compressive strength of the ice
F	MN	horizontal ice force

Table 17. Results of calculation

t, m	D,m	I	f_c	C_x, MPa	F, MN
0,5	100	1,2	0,55	2,5	83
0,6	100	1,2	0,55	2,5	99
0,7	100	1,2	0,55	2,5	116
0,8	100	1,2	0,55	2,5	132
0,9	100	1,2	0,55	2,5	149
1,0	100	1,2	0,55	2,5	165
1,1	100	1,2	0,55	2,5	182
1,2	100	1,2	0,55	2,5	198
1,3	100	1,2	0,55	2,5	215
1,4	100	1,2	0,55	2,5	231
1,5	100	1,2	0,55	2,5	248
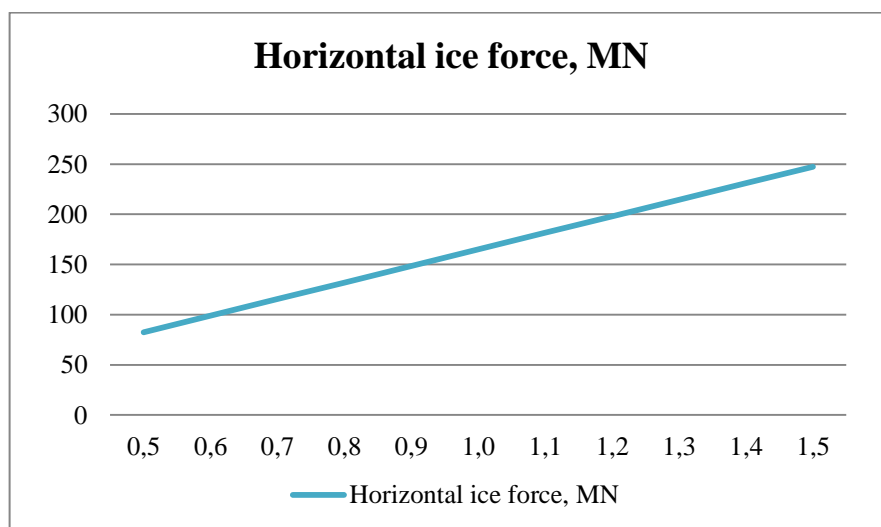
Figure 38. Horizontal force depending on ice thickness on vertical structure (API 2N RP)

2.1. Sheet or floe bending

Table 18. Description of the initial parameters for calculation of the horizontal and vertical ice force on the cone.

Parameter	Unit	Description
R_h	MN	horizontal force on the cone
R_v	MN	vertical force on the cone
p_w	kg/m^3	unit mass of water
σ	Pa	sheet ice bending strength
t	m	ice sheet thickness
$t_{ride\ up}$	m	ice ride up thickness
D	m	waterline diameter of the cone
D_t	m	top diameter of the cone
g	m/s^2	acceleration gravity

Table 19. Initial data for calculation of the horizontal and vertical ice force on the cone.

Parameter	Unit	Value
t	m	0,5
$t_{ride\ up}$	m	0,4
D_t	m	80
D	m	100
g	m/s^2	9,81
σ	Pa	2800000
p_w	kg/m^3	1025
f	-	72

Table 20. Coefficients defined from Figure 18.

Coefficient	Value
A_1	3,0
A_2	0,03
A_3	0,23
A_4	1,8
B_1	0,8
B_2	0,031

Table 21. Horizontal and vertical force in the cone.

Parameter	Unit	Value
R_h	MN	10,1
R_v	MN	8,5

APPENDIX C.

In the tables below (21, 22) are given the input data and results of determinations of ice loads by using ISO 19906. (see the Chapter 2)

Table 22. Description of the initial parameters for calculation of the global average ice pressure.

Parameter	Unit	Description
p_G	MPa	is the global average ice pressure
w	m	is the projected width of the structure
h	m	is the thickness of the ice sheet
h_1	m	is a reference thickness of 1 m
m	-	is an empirical coefficient equal to -0,16;
n	-	is an empirical coefficient, equal to $-0,50 + h/5$ for $h < 1,0$ m and to $-0,30$ for $h > 1$;
C_R	MPa	is the ice strength coefficient

Table 23. Results of the global average ice pressure calculation.

Ice thikness,m	w, m	h_1, m	m	n	C_r, MPa	Global average pressure, MPa
0,5	100	1	-0,16	-0,4	2,8	1,58
0,6	100	1	-0,16	-0,38	2,8	1,50
0,7	100	1	-0,16	-0,36	2,8	1,44
0,8	100	1	-0,16	-0,34	2,8	1,40
0,9	100	1	-0,16	-0,32	2,8	1,36
1,0	100	1	-0,16	-0,3	2,8	1,34
1,1	100	1	-0,16	-0,3	2,8	1,32
1,2	100	1	-0,16	-0,3	2,8	1,31
1,3	100	1	-0,16	-0,3	2,8	1,29
1,4	100	1	-0,16	-0,3	2,8	1,28
1,5	100	1	-0,16	-0,3	2,8	1,27
1,6	100	1	-0,16	-0,3	2,8	1,25
1,7	100	1	-0,16	-0,3	2,8	1,24
1,8	100	1	-0,16	-0,3	2,8	1,23
1,9	100	1	-0,16	-0,3	2,8	1,22
2,0	100	1	-0,16	-0,3	2,8	1,22
2,1	100	1	-0,16	-0,3	2,8	1,21
2,2	100	1	-0,16	-0,3	2,8	1,20
2,3	100	1	-0,16	-0,3	2,8	1,19
2,4	100	1	-0,16	-0,3	2,8	1,19
2,5	100	1	-0,16	-0,3	2,8	1,18
2,6	100	1	-0,16	-0,3	2,8	1,17
2,7	100	1	-0,16	-0,3	2,8	1,17
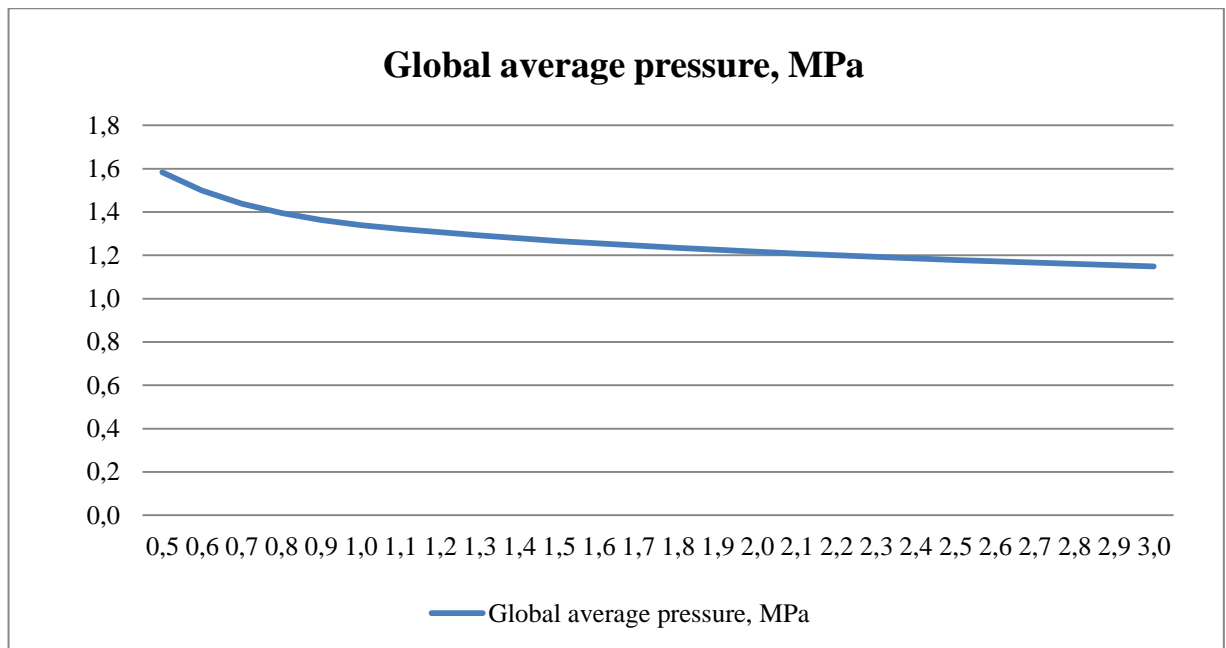
Figure 39. Global average ice pressure (ISO 19906).

Table 24. Description of the initial parameters for calculation horizontal and vertical component of ice action.

Parameter	Unit	Description
α	deg	slope of structure face from horizontal
h_r	m	is the ice ride-up thickness
h	m	is the thickness of the ice sheet
w_t	m	is the top diameter of the cone
w	m	is the waterline diameter of the cone or width of a sloping structure
μ	-	ice-structure friction coefficient
ρ_i	kg/m^3	is the density of ice
g	m/s^2	is the acceleration due to gravity
σ_f	MPa	is the flexural strength of the ice sheet
H_r	N	is the vertical action on cone due to ride-up
V_r	N	is the vertical action on cone due to ride-up
H_b	N	is the horizontal action on the cone due to ice breaking
V_b	N	is the vertical action on the cone due to ice breaking
F_H	N	horizontal component of ice action
F_V	N	vertical component of ice action

Table 25. Initial data for calculation of horizontal and vertical component of ice action.

Parameter	Unit	Value
α	deg	60
h_r	m	0,7
h	m	0,5
w_t	m	80
w	m	100
μ	-	0,3
ρ_i	kg/m^3	720
g	m/s^2	9,81
σ_f	MPa	2,5

Table 26. Result of intermediate calculations 1.

Parameter	Unit	Value
f	-	1,19
g_r	-	6,30
h_v	-	0,024
W	-	8899632
E_1	-	2,16
E_2	-	1,21
Y	-	2,71
X	-	1,15
G	-	14,12

Table 27. Result of intermediate calculations 2.

Parameter	Unit	Value
V_r	N	8474349,0
H_r	N	16347073,8
V_b	N	863622,2
H_b	N	526803,6

Table 28. Result of calculation of horizontal and vertical component of ice action.

Parameter	Unit	Value
F_H	MN	16,87
F_V	MN	9,34

APPENDIX D.

In the tables below (23-27) are given the input data and results of determinations of ice loads by using SNIP-2.06.04-82. (see the Chapter 2)

Table 29. Description of the initial parameters for calculation the ice load forces.

Parameter	Unit	Description
R_c	MPa	ice resistances in compression
t_a	∘C	average daily air temperature
R_f	MPa	ice resistances in bending
R_b	MPa	ice resistances in collapse
A	m^2	area of the ice field
h_d	m	estimated ice thickness
v	m/s	velocity of the ice floe
α	deg	inclination of the wall
m	-	the form factor in terms of support beam
m_t	-	coefficient taken from Table 6
k_b	-	coefficient taken from Table 5
b	m	width of structure
$F_{b,p}$	MN	force caused by the ice-field beam stop
$F_{c,w}$	MN	force caused by the impacted individual floes
$F_{b,w}$	MN	force caused by crushing
$F_{h,p}$	MN	a horizontal force component
$Fv_{,p}$	MN	a vertical force component

Table 30. Initial data for calculation of the ice load forces.

Parameter	Unit	Value
R_c	MPa	1,35
t_a	∘C	-30
R_f	MPa	0,675
R_b	MPa	1,35
b	m	100
h_d	m	0,5
b/h_d	-	200
m	-	1
A	m^2	10000
v	m/s	0,5

Table 31. Results of the ice loads calculations.

Parameter	Unit	Value
$F_{b,p}$	MN	101,25
$F_{c,w}$	MN	3,05
$F_{b,w}$	MN	50,63

Table 32. Initial data for horizontal and vertical forces calculation.

Parameter	Unit	Value
R_f	MPa	0,675
h_d	m	0,5
b	m	100
α	deg	60
m_t	-	1,73
k_b	-	40

Table 33. Results of horizontal and vertical forces calculation.

Parameter	Unit	Value
$F_{h,p}$	MN	11,6775
$Fv_{,p}$	MN	6,75

APPENDIX E.

In the tables below (28-31) are given the input data and results of determination of ice loads by using VSN 41.88. (see the Chapter 2)

Table 34. Initial data for ice load calculation on the vertical sided structure.

Parameter	Unit	Value
R_c	MPa	1,4
R_f	MPa	0,6
S	%	3
m_1	-	1
b	m	100
h_d	m	0,5
k_b	-	2,2
b/h_d	-	200

Table 35. Result of the ice load calculation on the vertical sided structure.

Parameter	Unit	Value
$F_{b,p}$	MN	154

Table 36. Initial data for ice load calculation on the sloped sided structure.

Parameter	Unit	Value
K_a	-	22
α	deg	30
R_f	MPa	0,6
h_d	m	0,5
f	-	0,3

Table 37. Results of the ice load on sloped sided structure.

Parameter	Unit	Value
F_v	MN	3,3
F_h	MN	12,08